The Minimizer of the Dirichlet Integral

Ruomeng Lan

A Thesis in

The Department of Mathematics

and Statistics

Presented in Partial Fulfillment of the Requirements for the Degree of Master of Science (Mathematics) at Concordia University

Montreal, Quebec, Canada

January 2012

CONCORDIA UNIVERSITY

School of Graduate Studies

This is to certify that the thesis prepared

By: Ruomeng Lan

Entitled: The Minimizer of the Dirichlet Integral

and submitted in partial fulfillment of the requirements for the degree of

Master of Science (Mathematics)

complies with the regulations of the University and meets the accepted standards with respect to originality and quality.

Signed by the final Examining Committee:

_____ Richard Hall_____ Chair

_____ Alina Stancu_____ Examiner

_____ Alexander Shnirelman_____ Examiner

_____ Alexander Shnirelman_____ Supervisor

Approved by _____ Jose Garrido_____

Chair of Department or Graduate Program Director

_____ Brian Lewis_____

Dean of Faculty

Date _____

Abstract

The Minimizer of the Dirichlet Integral

Ruomeng Lan

In this thesis, we consider the minimizer of the Dirichlet integral, which is used to compute the magnetic energy. We know that the Euler equations describe a motion of an inviscid incompressible fluid. We show that the infimum of the Dirichlet integral, by the action of area-preserving diffeomorphisms, is a stream function corresponding to some velocity field, which is a solution to the stationary Euler equation. According to this result, we study the properties and behaviors of the steady incompressible flow numerically. We utilize three distinct numerical methods to simulate the minimizer of the Dirichlet integral. In all cases the singularity formation was observed. Every hyperbolic critical point of the original function gives rise to a singularity of the minimizer.

Acknowledgements

First and foremost, I wish to thank my supervisor, Professor Alexander Shnirelman, for his guidance and help. I really appreciate all his contributions of time, ideas, and funding for my study and research at Concordia. It would not have been possible to write the master thesis without his support and his patience. I also thank him for his sense of humor and his interesting stories about mathematicians during our meetings.

I especially wish to thank my parents for all their love. They always provide encouragement and consolation throughout my life. I thank them for believing in me and supporting my pursuit. Mother and father, I love you.

Finally, I wish to thank my cousin, Angela Sun, and all my friends in Montreal. They made my life filled with fun and joy in last two years.

Contents

List of Figures

Chapter 1

Introduction

My thesis is devoted to the study of the Magnetic Equilibrium Problem. This problem appears in astrophysics (the solar corona, magnetized neutron stars), geophysics (terrestrial magnetism), nuclear engineering (plasma equilibrium in Tokamak), and other situations. In general, we consider an electrically conductive medium ("fluid") interacting with a magnetic field. If the electric conductance of the medium is high enough, and/or the size of the domain is large enough, the Ohmic resistance of the fluid is negligible, and the magnetic field is "frozen in"; it is transported by the fluid. On the other hand, the magnetic field produces a force upon the fluid affecting its motion. Thus, we have a system of interacting magnetic field and moving fluid; this system is described by the equations of MagnetoHydroDynamics (MHD) (see below). Here we can single out two extreme cases:

(1) The magnetic field is passively driven by the fluid, while its reverse action on the fluid is negligible; the fluid is driven by other forces, say by convection. This may result in the growth of magnetic field. Such situation is called "Magnetic Dynamo" and is regarded as a possible mechanism of generation of the terrestrial magnetic field.

(b) The fluid is driven exclusively by the magnetic field, while other moving forces are negligible. In this case the magnetic field tends to assume a configuration having

minimal magnetic energy. This is the magnetic equilibrium problem called sometimes the Sakharov-Zeldovich problem.

This is an extremely nonlinear, degenerate problem; it may be regarded as a degenerate problem of nonlinear elasticity. The prominent feature of such problems is the formation of singularities in the course of minimization. The nature of these singularities is the most interesting question in the study of the problem. I restrict the study to the case of a field frozen in an incompressible 2-dimensional fluid in a compact domain M. This is a considerable simplification, but even in this model case some characteristic singularities are observed. The central role in our work is played by the classical observation that any energy minimizing configuration of magnetic field may be regarded as a velocity field of a steady (time independent) solution of 2-d Euler equations describing the flow of ideal incompressible fluid.

My thesis contains two main parts, theoretical analysis and numerical analysis. In chapter 2, the theoretical part, we begin with introducing the Euler equations, following [2]. We will explain the equations from the mathematical and physical viewpoints. Then we define the vorticity field ω and state the interpretation and some properties (also see [3]) of vorticity. Meanwhile, we introduce the stream function and show the uniqueness of solution of the Euler equations equipped with a vorticity field in a simply connected domain. We also introduce the steady Euler equations whose solutions do not depend on the time. The solutions are good models to study the fluid equilibrium or the motion after a long period of time. Theorem 3 states a property of the stream functions corresponding to the solutions of steady Euler equations, which is a crucial result for the numerical part. The last section in chapter 2 is about the magnetodydrodynamics [1, 4, 13]. We state two variation problems from [1] and provide the definition of Dirichlet integral. Theorem 4 shows the equivalence between the minimizer of the Dirichlet integral and the stream function of steady Euler equation, which is the theoretical fundament of the numerical part.

In chapter 3, we find the minimizer of the Dirichlet integral by three dinstinct numerical methods. All the methods employ the idea of the penalty function [6, 7]. The finite element method is the most used for the computing the integral numerically; the water bag method can preserve the area better and obtain more details about the level lines of the minimizer near the singularity line and the method of bubbles with level lines can provide a panoramic view of the minimizer directly.

Chapter 2

Theoretical Analysis

2.1 Euler Equation

Fluid mechanics is the study of behavior of gases and liquids. The phenomena studied in this thesis are macroscopic. In other words, we only focus on the gross behavior of many molecules constituting the fluid, instead of an individual molecule. For this purpose we regard the fluid as a continuum, a point of which is a very small portion of the real fluid, negligible with respect to the macroscopic size, but very large with respect to the intermolecular distance. This small volume, a point of continuum, is called *fluid particle*. Consequently, the physical state of a fluid will be described by properties of the fluid particles and not by the physical state of all the microscopic molecules. The macroscopic fields describing the state, such as the velocity field $u = u(x)$, the density field $\rho = \rho(x)$, can be physically interpreted by means of averages of suitable microscopic quantities. For example, the macroscopic velocity field at a point $u(x)$ means

$$u(x) = \frac{1}{N(x)} \sum_{i=1}^{N(x)} \mu_i \tag{2.1}$$

where $N(x)$ is the number of molecules associated to the fluid particle localized in x and μ_i, $i = 1, ..., N(x)$ are the velocities of these molecules.

In this thesis, we will mainly use the *Euler Equation* to study the properties of inviscid incompressible flow.

Let $M \subset \mathbb{R}^n$ (usually n=2 or 3) be an open and bounded set with a regular boundary ∂M containing a fluid represented as a continuum of particles. We can define a kind of displacements in the domain.

Definition 1. *An **incompressible displacement** of the fluid is a transformation $s : M \to M$ satisfying the following properties:*

(a) s is invertible and $s(M) = M$;

(b) $s, s^{-1} \in C^1(M)$; and

(c) s preserves the Lebesgue measure.

The property (a) means s should be bijective and the range is just the domain itself; in (b) C^1 denotes the set of continuous functions with continuous derivatives and the the property (c) means that, for any measurable set A the set $A \subset M$ defined by

$$s(A) = \{x \in M | s^{-1}(x) \in A\}, \tag{2.2}$$

we have

$$|s(A)| = |A| \tag{2.3}$$

where $|A|$ =mes A denotes the Lebesgue measure of A. We denote by S the set of all the incompressible displacements. It is evident that S has a group structure with respect to the law of natural compostition

$$s_1 \circ s_2(x) = s_1(s_2(x)). \tag{2.4}$$

Definition 2. *An **incompressible motion** is a function $s,\ t \in R^1 \to \Phi_{s,t} \in S$ such that:*

(a) $\Phi_{s,t}(\Phi_{t,r}(x)) = \Phi_{s,r}(x)$;

(b) $\Phi_{t,t}(x) = x$*; and*

(c) $\Phi_{t,s}$ *is continuously differentiable in* t *and* s*.*

Here $\Phi_{s,t}$ denotes the position at time t of the particle of fluid, which was at the point x at s. All these conditions are reasonable properties of regularity. The requirement that the transformation be invertible implies that one particle of fluid cannot occupy the position of a distinct particle.

Now we denote by $\rho = \rho(x,t)$ the *density field*. Then we can compute the mass of fluid contained in the element of volume dx as $\rho(x,t)\,dx$. Here we assume that $\rho \in C(D)$. By the law of conservation of mass (see [5]), we have

$$\frac{d}{dt}\int_{V_t} \rho(x,t)\,dx = 0 \tag{2.5}$$

where

$$V_t = \{\Phi_t(x) | x \in V_0\} \tag{2.6}$$

is the region moving along the trajectories of an incompressible motion and the trajectory function $\Phi_t(x) = \Phi_{t,0}(x)$

Let

$$u(\Phi_t(x), t) = \frac{d}{dt}\Phi_t(x) \tag{2.7}$$

be the velocity field associated with this motion. Then, by (2.5), we have

$$\begin{aligned}\frac{d}{dt}\int_{V_t} \rho(x,t)\,dx &= \frac{d}{dt}\int_{V_0} \rho(x,t)J_t(x)\,dx \\ &= \frac{d}{dt}\int_{V_0} \rho(x,t)\,dx = 0\end{aligned} \tag{2.8}$$

where $J_t(x)$ is the Jacobian of the transformation $x \to \Phi_t(x)$ and the value is one by the incompressibility condition (see [2]).

Hence, by the arbitrariness of V_0, we have

$$\frac{d}{dt}\rho(\Phi_t(x), t) = 0 \tag{2.9}$$

which means the density is constant.

The condition of incompressibility is equivalent, by the Liouville Theorem (see [8]), to the condition

$$\text{div } u(x,t) = 0, \qquad \forall x \in M, \quad t \in \mathbb{R}. \tag{2.10}$$

Equation (2.10) is usually called the continuity equation for incompressible flows. We call the vector field satisfying (2.10) *divergence-free* field.

Since the particles cannot pass through the boundary,

$$u(x,t) \cdot n = 0 \qquad \text{on } \partial M, \tag{2.11}$$

where n is the exterior unit normal (this is called a *slip condition*).

We use the notation

$$D_t f \equiv \partial_t f + (u, \nabla) f \tag{2.12}$$

for the derivative of a function f along the trajectories $\Phi_t(x)$. In this case we have

$$D_t u = -\nabla p \tag{2.13}$$

where p is a scalar function. The physical meaning of the equation is that the acceleration of a fluid particle, $D_t u$, is equal to a force $-\nabla p$. From another point, $-\nabla p$ can be consider as the constraint force for a free partical system constrained to move on a manifold. The scalar field $p = p(x,t)$ is called *pressure*.

Together with Equation (2.10) and (2.11) we obtain the *Lagrange-Euler equation* for an ideal (inviscid) incompressible fluid

$$\begin{aligned} D_t u &= -\nabla p \\ \text{div } u &= 0 \\ u \cdot n &= 0 \quad \text{on } \partial M \end{aligned}$$

If we consider $M \in \mathbb{R}^2$, and substitute D_t from the previous equation, then we obtain the Euler equations for the velocity and pressure fields which look as follows:

$$\frac{\partial}{\partial x_i} u_i(x,t) + \sum_{j=1}^{2} u_j \frac{\partial}{\partial x_j} u_i(x,t) = -\frac{\partial}{\partial x_i} p(x,t) \quad i = 1,2 \tag{2.14}$$

$$\frac{\partial}{\partial x_1} u_1(x,t) + \frac{\partial}{\partial x_2} u_2(x,t) = 0 \tag{2.15}$$

$$u_1 n_1 + u_2 n_2 = 0 \quad \text{on } \partial M \tag{2.16}$$

where $u = (u_1, u_2)$ and $n = (n_1, n_2)$.

2.2 Vorticity and Stream Function

Now consider another important field, the *vorticity field* $\omega(x)$.

Definition 3.

$$\omega(x) \equiv \text{curl}\, u \equiv \nabla \times u \tag{2.17}$$

The vorticity field $\omega(x)$ is a measure of the fluid rotation. We can understand the meaning of ω in the following way. Every smooth velocity field $u(x,t)$ has a Taylor series expansion at a fixed point x_0

$$u(x_0 + h) = u(x_0) + (\nabla u)(x_0)h + O(h^2), \tag{2.18}$$

where ∇u is a matrix

$$(\nabla u)_{ij} = \frac{\partial u_i}{\partial x_j}. \tag{2.19}$$

Moreover, ∇u has a symmetric part D and an antisymmetric part Ω:

$$D = \frac{1}{2}(\nabla u + \nabla u^T) \tag{2.20}$$

$$\Omega = \frac{1}{2}(\nabla u - \nabla u^T). \tag{2.21}$$

D is called the deformation matrix and Ω is called the rotation matrix. Since the flow is incompressible, div $u = 0$, then the trace tr $D = 0$. We can also find that ω satisfies

$$\Omega \cdot h = \frac{1}{2}\omega \times h \tag{2.22}$$

Using the Taylor series expression (2.18), the definitions of D and ω we have

$$u(x_0 + h) = u(x_0) + \frac{1}{2}\omega \times h + D \cdot h + O(h^2). \tag{2.23}$$

From (2.23) we see that the velocity of a point close to x_0 is the sum of three terms: a translation, a rotation with angular velocity $\frac{1}{2}\omega$ and a deformation.

Now let $M \subset \mathbb{R}^3$. By (2.17) we have

$$\omega(x) = (\frac{\partial u_3}{\partial x_2} - \frac{\partial u_2}{\partial x_3}, \frac{\partial u_1}{\partial x_3} - \frac{\partial u_3}{\partial x_1}, \frac{\partial u_2}{\partial x_1} - \frac{\partial u_1}{\partial x_2}) \tag{2.24}$$

By observation, we will find that if the $M \subset \mathbb{R}^2$, then ω is a scalar field because only the third component of curl does not vanish. In this case, we also denote this third component as curl u.

We can pose the following problem by using the vorticity field to study the behavior of fluids. If the vorticity field ω is known, we want to deduce the velocity field u generating ω. So we should solve the following equations in the unknown quantity

u

$$\operatorname{curl} u = \omega, \quad \operatorname{div} u = 0 \tag{2.25}$$

where we let the given field $\omega \in C(M)$.

Now we consider the system in 2-dimension. Equations (2.25) can be rewritten as

$$\frac{\partial u_2}{\partial x_1} - \frac{\partial u_1}{\partial x_2} = \operatorname{curl} u = \omega \tag{2.26}$$

$$\frac{\partial u_1}{\partial x_1} + \frac{\partial u_2}{\partial x_2} = 0 \tag{2.27}$$

However, the solution of the system of Equations (2.26) and (2.27) may not be unique. In fact, if u' is a solution of the system, then $u = u' + \nabla\varphi$, where φ is a harmonic function, is a solution as well. Thus, we add Equation (2.11), the boundary condition, to obtain a unique solution.

Now we restrict that M is simply connected and bounded. In this case, the condition div $u = 0$ allows us to introduce a function Ψ such that

$$u = \nabla^{\perp}\Psi \tag{2.28}$$

where

$$\nabla^{\perp} = (\frac{\partial}{\partial x_2}, -\frac{\partial}{\partial x_1}) \tag{2.29}$$

is called the skew gradient.

Definition 4. *The function Ψ, satisfying the equation* (2.28)*, is called the* ***Stream Function****.*

By the definition of ω we have

$$\Delta\Psi = -\omega \tag{2.30}$$

Equation (2.30) is called the Poisson equation (see [9]).

From the condition $u \cdot n = 0$ on ∂M, it follows that Ψ must be a constant on ∂M. For convenience, we suppose

$$\Psi|_{\partial M} = 0. \tag{2.31}$$

Theorem 1. *Equations* (2.26) *and* (2.27) *with the condition* $u \cdot n = 0$ *have a unique solution.*

Proof. Suppose the equations have two distinct solutions u and u' and let $v = u - u'$. We should only show that $v = 0$. Since u and u' are both solutions of equations (2.26) and (2.27), then we have

$$\text{div } v = \text{div } (u - u') = 0, \quad \text{curl } v = \text{curl } (u - u') = 0$$

From the second equation, we have

$$\frac{\partial v_2}{\partial x_1} - \frac{\partial v_1}{\partial x_2} = 0.$$

Because the domain M is simply connected, there exists a function φ such that

$$v = \nabla \varphi. \tag{2.32}$$

Since $v \cdot n = 0$ on ∂M, then $\frac{\partial}{\partial n}\varphi = 0$ on ∂M. Taking the divergence of (2.32) we obtain the Neumann problem

$$\begin{aligned} \Delta \varphi &= 0 \\ \frac{\partial}{\partial n}\varphi &= 0 \quad \text{on } \partial M \end{aligned}$$

The only solution for this problem implies that φ is a constant function. It follows that $v = 0$ on M. □

2.3 Steady Euler Equation

Now let us consider the corresponding idealized model of steady flows of an incompressible fluid. Such flows are stationary solutions of Euler equation that do not depends on time.

Definition 5. *An ideal **steady** (or **stationary**) incompressible fluid flow $u(x)$ in a domain $M \subset \mathbb{R}^n$ is a divergence-free solution, namely div $u = 0$ of the **steady Euler equation***

$$(u, \nabla)u = -\nabla p \tag{2.33}$$

where p denotes some pressure function on M.

Comparing with (2.13), equation (2.33) does not contain the component $\partial_t u$. Thus, as mentioned, the solutions of (2.33) does not depend on time. The following theorem describes a property of the solutions of (2.33) when $M \subset \mathbb{R}^3$.

Theorem 2. *If $u(x)$ is a solution of equation* (2.33) *in $M \subset \mathbb{R}^3$, then we have*

$$u \times \operatorname{curl} u = \nabla \alpha \tag{2.34}$$

where $\alpha = p + \frac{\|u\|^2}{2}$

We will prove it in Cartesian coordinates.

Proof. Suppose first $u = (u_1, u_2, u_3)$. Then we have

$$\operatorname{curl} u = (\frac{\partial u_3}{\partial x_2} - \frac{\partial u_2}{\partial x_3}, \frac{\partial u_1}{\partial x_3} - \frac{\partial u_3}{\partial x_1}, \frac{\partial u_2}{\partial x_1} - \frac{\partial u_1}{\partial x_2}) \tag{2.35}$$

Then the left side of (2.34) is

$$\begin{aligned} u \times \operatorname{curl} u =&(u_2(\frac{\partial u_2}{\partial x_1} - \frac{\partial u_1}{\partial x_2}) - u_3(\frac{\partial u_1}{\partial x_3} - \frac{\partial u_1}{\partial x_3}), u_3(\frac{\partial u_1}{\partial x_3} - \frac{\partial u_3}{\partial x_1}) - u_1(\frac{\partial u_2}{\partial x_1} - \frac{\partial u_1}{\partial x_2}),\\ & u_1(\frac{\partial u_1}{\partial x_3} - \frac{\partial u_3}{\partial x_1}) - u_2(\frac{\partial u_3}{\partial x_2} - \frac{\partial u_2}{\partial x_3})) \end{aligned}$$

After rewriting, we have

$$\begin{aligned} u \times \operatorname{curl} u =& - (u_1\frac{\partial u_1}{\partial x_1} + u_2\frac{\partial u_1}{\partial x_2} + u_3\frac{\partial u_1}{\partial x_3}, u_1\frac{\partial u_2}{\partial x_1} + u_2\frac{\partial u_2}{\partial x_2} + u_3\frac{\partial u_2}{\partial x_3},\\ & u_1\frac{\partial u_3}{\partial x_1} + u_2\frac{\partial u_3}{\partial x_2} + u_3\frac{\partial u_3}{\partial x_3})+\\ & (u_1\frac{\partial u_1}{\partial x_1} + u_2\frac{\partial u_2}{\partial x_1} + u_3\frac{\partial u_3}{\partial x_1}, u_1\frac{\partial u_1}{\partial x_2} + u_2\frac{\partial u_2}{\partial x_2} + u_3\frac{\partial u_3}{\partial x_2},\\ & u_1\frac{\partial u_1}{\partial x_3} + u_2\frac{\partial u_2}{\partial x_3} + u_3\frac{\partial u_3}{\partial x_3})\\ =& - (\sum_{i=1}^{3} u_i\frac{\partial u_1}{\partial x_i}, \sum_{i=1}^{3} u_i\frac{\partial u_2}{\partial x_i}, \sum_{i=1}^{3} u_i\frac{\partial u_3}{\partial x_i})+\\ & (\sum_{i=1}^{3} u_i\frac{\partial u_i}{\partial x_1}, \sum_{i=1}^{3} u_i\frac{\partial u_i}{\partial x_2}, \sum_{i=1}^{3} u_i\frac{\partial u_i}{\partial x_3})\\ =& - (u, \nabla)u + \nabla(\frac{\|u\|^2}{2}) \end{aligned}$$

By equation, (2.33) we know that $-(u, \nabla)u = \nabla p$. Thus, we obtain the equation (2.34). □

Definition 6. *The function α: $M \to \mathbb{R}$ defined by the relation $u \times \operatorname{curl} u = \nabla\alpha$ is called the* ***Bernoulli function*** *of the steady flow u.*

Recall that the vorticity $\omega = \operatorname{curl} u$. So (2.34) can be rewritten as $u \times \omega = \nabla\alpha$. It follows that both of the velocity field and vorticity field are tangent to the level surfaces of the Bernoulli function α.

If $M \subset \mathbb{R}^2$, we can obtain a stronger result.

Theorem 3. *Let Ψ be the stream function corresponding to $u(x)$ which is the solution*

of (2.33) *in* $M \subset \mathbb{R}^2$. *Then we have the equation*

$$\nabla\Psi \times \nabla\Delta\Psi = 0 \tag{2.36}$$

Proof. Take the operation $\nabla^\perp$ on both sides of (2.33). Then the right side is

$$\nabla^\perp(\nabla p) = \frac{\partial^2 p}{\partial x_2 \partial x_1} - \frac{\partial^2 p}{\partial x_1 \partial x_2} = 0 \tag{2.37}$$

and the left side is

$$\begin{aligned}\nabla^\perp((u,\nabla)u) =&(\frac{\partial u_1}{\partial x_2}\frac{\partial u_1}{\partial x_1} + u_1\frac{\partial^2 u_1}{\partial x_1 \partial x_2} + \frac{\partial u_2}{\partial x_2}\frac{\partial u_1}{\partial x_2} + u_2\frac{\partial^2 u_1}{\partial x_2^2})-\\ &(\frac{\partial u_1}{\partial x_1}\frac{\partial u_2}{\partial x_1} + u_1\frac{\partial^2 u_1}{\partial x_1^2} + \frac{\partial u_2}{\partial x_1}\frac{\partial u_2}{\partial x_2} + u_2\frac{\partial^2 u_1}{\partial x_2 \partial x_1})\\ =&(u_1\frac{\partial^2 u_1}{\partial x_1 \partial x_2} + u_2\frac{\partial^2 u_1}{\partial x_2^2}) - u_1\frac{\partial^2 u_1}{\partial x_1^2} - u_2\frac{\partial^2 u_1}{\partial x_2 \partial x_1}+\\ &(\frac{\partial u_1}{\partial x_2} - \frac{\partial u_2}{\partial x_1})\mathrm{div}\, u\end{aligned}$$

Since $\mathrm{div}\, u = 0$, we obtain

$$u_1\frac{\partial^2 u_1}{\partial x_1 \partial x_2} + u_2\frac{\partial^2 u_1}{\partial x_2^2} - u_1\frac{\partial^2 u_1}{\partial x_1^2} - u_2\frac{\partial^2 u_1}{\partial x_2 \partial x_1} = 0 \tag{2.38}$$

We know $u = \nabla^\perp\Psi$. Then we have

$$\nabla\Psi = (-u_2, u_1), \quad \Delta\Psi = -\omega = -\frac{\partial u_2}{\partial x_1} + \frac{\partial u_1}{\partial x_2} \tag{2.39}$$

We can compute the left side of (2.36) by using u

$$\nabla\Psi \times \nabla\Delta\Psi = u_1\frac{\partial^2 u_1}{\partial x_1 \partial x_2} + u_2\frac{\partial^2 u_1}{\partial x_2^2} - u_1\frac{\partial^2 u_1}{\partial x_1^2} - u_2\frac{\partial^2 u_1}{\partial x_2 \partial x_1} \tag{2.40}$$

which is just the left side of (2.38). Thus, equation(2.36) holds when $M \subset \mathbb{R}^2$. □

2.4 Magnetic Equilirium

The study of the fluid which is electrically conducting and moves in a magnetic field is known as *Magnetohydrodynamics* or MHD for short. The simplest example of an electrically conducting fluid is a liquid metal, for example, mercury or liquid sodium (see [10]). However, the major use of MHD is in plasma physics (see [11] and [12]). A plasma is a hot, ionized gas containing free electrons and ions. It is not obvious that plasmas can be regarded as fluids since the mean free paths for collisions between the electrons and ions are macroscopically long. But when we consider the large number of plasma particles, the collective interactions between them can isotropize the particles velocity distributions in some local mean reference frame, thereby making it sensible to describe the plasma macroscopically by a mean density, velocity, and pressure. These mean quantities can then be shown to obey the same conservation laws of mass, momentum and energy, as derived for fluids (see [13]).

Now we consider the governing equations of MHD. Suppose the domain $M \subset \mathbb{R}^3$ is filled with an electrically conducting fluid, which is incompressible with respect to the standard volume form $\mu = d^3x$ and transports a divergence-free magnetic field $\mathbf{B}$. Then, the evolution of the field $\mathbf{B}$ and of the fluid velocity field v is described by the system of ideal *magnetohydrodynamics equations* [1]

$$\begin{cases} \frac{\partial v}{\partial t} = -(v, \nabla)v + (\text{curl } \mathbf{B} \times \mathbf{B}) - \nabla p \\ \frac{\partial \mathbf{B}}{\partial t} = -\{v, \mathbf{B}\} \\ \text{div } \mathbf{B} = 0 \end{cases} \tag{2.41}$$

In the first equation of (2.41) the pressure term ∇p is uniquely defined by the condition $\partial v/\partial t = 0$, just as it is for the Euler equation in ideal hydrodynamics. The term curl $\mathbf{B} \times \mathbf{B}$ represents the Lorentz force. The second equation is the definition of the "frozenness" of the magnetic field $\mathbf{B}$ into the medium, and $\{,\}$ denotes the Poisson

bracket (see [14]) space of two vector fields.

The total energy $\mathbb{E}$ of the MHD system is the sum of the kinetic and magnetic energy

$$\mathbb{E} := \frac{1}{2}\int_M (v,v)\mu + \frac{1}{2}\int_M (\mathbf{B},\mathbf{B})\mu \tag{2.42}$$

where $(,)$ denotes the inner product of two vectors.

Recall the Bernoulli function α and equation (2.34). If α is constant, then we have

$$u \times \text{curl} \equiv 0 \tag{2.43}$$

It follows that the velocity field u and the corresponding vorticity field ω are collinear at each point. In magnetohydrodynamics, such fields are called *force-free* fields.

Now we will focus only on the magnetic part of the total energy of the MHD system. Consider the following variational problem. Let M be a closed Riemannian manifold in $\mathbb{R}^3$ equipped with a volume form μ, and a divergence-free vector field ξ on M. The energy of the field is the integral

$$E = \frac{1}{2}\int_M (\xi,\xi)\mu. \tag{2.44}$$

Problem 1. *Find the minimum energy and the extremals among all fields obtained from a given field ξ by the action of volume-preserving diffeomorphisms of the manifold M.*

Denote the divergence-free field after the action of a volume-preserving diffeomorphism $g : M \to M$ on ξ, a divergence-free field, by ξ_g. Here g should satisfy the following condition: the flux of the field ξ across any surface σ is equal to the flux of ξ_g across $g(\sigma)$. In other words, the field is frozen into an incompressible fluid filling M: the vector field can be thought of as drawn on the elements of fluid and expanding as these elements expand. Moreover, for the boundary ∂M the field ξ is assumed to

be tangent to ∂M and the diffeomorphisms send the boundary ∂M into itself.

In magnetohydrodynamics, where this variational problem naturally arises, the role of ξ is played by a magnetic field B, frozen into a fluid of infinite conductivity filling M.

The above energy minimization problem assumes the following form of the Dirichlet problem in the two-dimensional case. Let M be a Riemannian Manifold in $\mathbb{R}^2$ with a Riemannian volume form μ.

Problem 2. *Find the infimum and the minimizer of the* ***Dirichlet integral***

$$E(u) = \frac{1}{2}\int_M (\nabla f, \nabla f)\mu \tag{2.45}$$

among all the smooth function f on the manifold M that can be obtained from a given function f_0 by the action of area-preserving diffeomorphisms of M to itself.

Both of the problems above arose in [1]. It is not hard to see that this is the two-dimensional version of Problem 1. We can consider the skew gradient $\nabla^\perp f$ instead of ∇f. This is because

$$(\nabla^\perp f, \nabla^\perp f) = (f_x)^2 + (f_y)^2 = (\nabla f, \nabla f) \tag{2.46}$$

where we consider them in the x, y coordinates. It follows that the functional E has the same value. Then f is regarded as a Hamiltonian function and any area-preserving change of coordinates for the function f implies the corresponding diffeomorphism action on the field $\nabla^\perp f$.

Theorem 4. *A smooth minimizer u of the Dirichlet Problem 2 on a Riemannian manifold M obeys the following condition: the gradient of the functions f and Δf are collinear at every point of M.*

We will prove the theorem above in X, Y coordinates.

Proof. To prove the theorem, we should only show that

$$\nabla f \times \nabla \Delta f \equiv 0. \tag{2.47}$$

Let δE be the first variation of the integral. Then we have

$$\begin{aligned}
\delta E &= \delta(\frac{1}{2}\int_M |\nabla f|^2 \,\mu) \\
&= \frac{1}{2}\int_M |\nabla(f+\delta f)|^2 - |\nabla f|^2 \mu \\
&= \frac{1}{2}\int_M |\nabla f|^2 + 2\nabla f \cdot \nabla \delta f + |\nabla \delta f|^2 - |\nabla f|^2 \,\mu \\
&= \int_M \nabla f \cdot \nabla \delta f \,\mu.
\end{aligned}$$

Suppose $\delta f = \epsilon \nu \cdot \nabla f$ where $\nu = \nabla^{\perp}\psi$ and $\psi = 0$ on ∂M. So we can rewrite the variation of the integral as

$$\begin{aligned}
\delta E &= \int_M \nabla f \cdot \nabla(\nu \cdot f)\,\mu \\
&= \int_{\partial M} (\nu \cdot \nabla f)\nabla f \cdot \overrightarrow{n}\, dS - \int_M (\nu \cdot \nabla f)\Delta f \,\mu \\
&= -\int_M (\nu \cdot \nabla f)\Delta f \,\mu \\
&= -\int_M (\nabla^{\perp}\psi \cdot \nabla f)\Delta f \,\mu
\end{aligned}$$

Here we use the first Green's identity and $\overrightarrow{n}$ is the outward normal of the boundary element dS. Since ν is zero on the boundary ∂M, we can neglect the first term. Now

express the integral $\int_M (\nabla^\perp \psi \cdot \nabla f)\Delta f \mu$ in coordinates as

$$\begin{aligned}\int_M (\nabla^\perp \psi \cdot f)\Delta f\, \mu &= \iint_M (\psi_y f_x - \psi_x f_y)(f_{xx} + f_{yy})\, dxdy \\ &= \iint_M \psi_y f_x (f_{xx} + f_{yy}) - \psi_x f_y (f_{xx} + f_{yy})\, dxdy \\ &= \int_{\partial M} \psi f_x (f_{xx} + f_{yy}) n_y\, dS - \int_{\partial M} \psi f_y (f_{xx} + f_{yy}) n_x\, dS \\ &\quad - \iint_M \psi f_{xy}(f_{xx} + f_{yy}) - \psi f_x (f_{xxy} + f_{yyy})\, dxdy \\ &\quad + \iint_M \psi f_{xy}(f_{xx} + f_{yy}) + \psi f_y (f_{xxx} + f_{yyx})\, dxdy\end{aligned}$$

where n_x and n_y are the components of the vector $\overrightarrow{n}$. Since $\psi = 0$ on the boundary ∂M, we have

$$\begin{aligned}\int_M (\nabla^\perp \psi \cdot f)\Delta f\, \mu &= -\int_M \psi (f_x (f_{xxy} + f_{yyy}) - f_y (f_{xxx} + f_{yyx}))\, dxdy \\ &= -\int_M \psi (\nabla f \times \nabla \Delta f)\, \mu.\end{aligned}$$

Thus, the variation of the integral (2.45) can be expressed as

$$\delta E = \int_M \psi (\nabla f \times \nabla \Delta f)\, \mu. \tag{2.48}$$

If the integral reaches a minimum at f, then the corresponding $\delta E(f) = 0$. Then $\int_M \psi (\nabla f \times \nabla \Delta f)\, dM = 0$. Since ψ is any functions such that $\psi|_{\partial M} = 0$, we have the identity (2.47)

$$\nabla f \times \nabla \Delta f \equiv 0.$$

□

We should note that equation (2.47) is the same as the equation (2.36). It means that if the integral reaches the minimum at the point f, then f is the stream function corresponding to some velocity field, which is a solution of the stationary Euler

equation. Thus, we can use the infimum of the Dirichlet energy (Problem 2) to study the properties and behaviors of the steady incompressible flow.

In the following numerical simulation, we will consider the function $f_g(x) = f(g^{-1}(x))$ for all area preserving diffeomorphisms g of the domain M. Instead of $E(f)$, the Dirichlet integral of the original function f, we consider $E(f_g)$, the Dirichlet integral of the transformed function $f_g = f \circ g^{-1}$. Then we will minimize $E(f_g)$ with respect to g. We use the result in [15], in which the existence of a weak solution of the minimization problem is proved. Such solutions admit transformations g which can be discontinuous along level lines of the function f. We want to show that the minimizer of the Dirichlet problem for an initial function with more than one critical point (for example, two maxima and a saddle point) has a singular line. We will call this phenomenon X-Y transition.

Chapter 3

Numerical Analysis

In this chapter, we will use numerical methods to solve **Problem 2** for several different functions $f(x)$. Namely, given a function $f(x)$, we consider functions $f_g(x) = f \circ g^{-1}(x)$ where g is an arbitrary area preserving diffeomorphism of M. We are looking for a function of this kind such that the Dirichlet integral $\int_M |\nabla f(x)|^2 dx$ is minimal. We use three different numerical methods to attack this problem. Each method has its advantages and disadvantages.

3.1 Finite Element Method

Finite element method, or FEM for short, is a very common numerical technique for computing the approximate solutions of partial differential equations and integral equations. In the finite element method, a continuous system to be analysed is divided into a number of discrete elements. Usually, the number should be very large to guarantee the accuracy of the corresponding numerical solution. Although the domain of the complete system may be very complex and irregular, each element is not difficult to analyze. According to the shape of the domain, the divisions into the elements may be different. However, in general, triangles and quadrilaterals are used in 2-D problem, and tetrahedrons and hexahedrons are used in 3-D problem.

So, the 2-dimensional domain M is divided into triangles Δ_i with the vertices $_i, B_i, C_i$. The function f is approximated by a function $\tilde{f}$ which is linear inside each triangle, and continuous in M. The diffeomorphism g is replaced by a continuous, piecewise-linear map $\tilde{g}$ which is linear inside every triangle Δ_i. In what follows we drop tilde and write simply f, g instead of $\tilde{f}$, $\tilde{g}$.

To define a piecewise linear map g, it is enough to define it for the vertices A_i, B_i, C_i of the triangles Δ_i, for they are extended inside the triangle by linearity. The same is true for the function f. The map g transforms every triangle Δ_i into another triangle Δ_i' with the vertices A_i', B_i', C_i', and the function f_g is uniquely defined by $f_g(A_i') = f(A_i), f_g(B_i') = f(B_i), f_g(C_i') = f(C_i)$, and then extended linearly inside M_i'.

So, the only variables of our problem (after we fix the vertices A_i, B_i, C_i of the triangles Δ_i and the initial function f at the same vertices) are the coordinates of the transformed triangles $\Delta_i' = g(\Delta_i)$. However, the choice of new triangles is not arbitrary, because the transformation g should be area-preserving. The obvious approximation to this condition for the discrete problem is the requirement that the area of any transformed triangle Δ_i' equals to the area of Δ_i for all i. But this requirement is too restrictive, and in what follows we will use softer methods to approximate the incompressibility.

Here we use the finite element method to evaluate Dirichlet energy

$$\mathscr{I}(g) = \frac{1}{2}\int_M |\nabla f_g(x)|^2 dx \tag{3.1}$$

in the domain M. But it should be noted that the volume (area in 2-D) of each triangle Δ_i may change during the progress of numerical minimization. Thus, we assume the fluid to be studied to be slightly compressible, in other words, the density is not constant, but can change slightly. When we minimize the energy of (3.1), we should consider the energy of density change.

Definition 7. *The energy of density change is defined as*

$$\mathscr{F}(g) = \int_M P\Big(\Big|\frac{\partial g(x)}{\partial x}\Big|\Big)dx \tag{3.2}$$

where $P(t)$ should satisfy that $P(1) = 0$ and $P(t) > 0$ when $t \neq 1$.

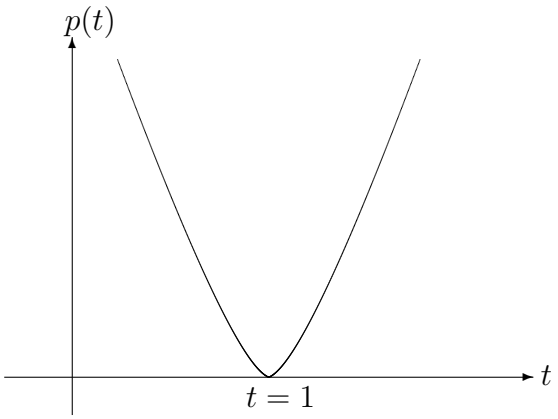

Figure 3.1: The Graph of $P(t)$

By the definition above, we know if the area does not change, then $\left|\frac{\partial g(x)}{\partial x}\right| = 1$, namely $\mathscr{F}(g) = 0$ as well.

We convert **Problem 2** into the minimization problem of the following function

$$\mathscr{E}(g) = \mathscr{I}(g) + \lambda\mathscr{F}(g) \tag{3.3}$$

where λ is a positive parameter. In this case, we should minimize the magnetic energy combined with the energy of density change. If λ is small (say $0 < \lambda < 1$), the object to be studied is a "small-soft" flow; if λ is large (say $\lambda \gg 1$), the flow is nearly incompressible. Thus, the second part guarantees that $g(x)$ is "almost" in SDiff (M) (the set of all area preserving diffeomorphisms of M). Actually, we can consider $\mathscr{F}$ and λ as the *penalty function* and the *penalty parameter*, respectively.

We should note that it is very crucial to set the value of λ. This is because, on one hand, the large λ can make $g(x)$ "more like" an area preserving diffeomorphism, on the

other side, if the λ is too large, the weight of the minimization for the magnetics energy will be decreased, in other words, we cannot approach very close to the minimizer for **Problem 2**.

Let us compute the energy of (3.3) by finite element method. We use a small triangle as the element in the computational method. Suppose that the vertices of the small triangle are A(x_1, y_1), B(x_2, y_2) and C(x_3, y_3), as in figure 3.2, and the corresponding values of the function f are

$$f(A) = \alpha, \quad f(B) = \beta, \quad f(C) = \gamma.$$

We should note that the function to be considered is $f_g(x) = f(g^{-1}(x))$, so the values

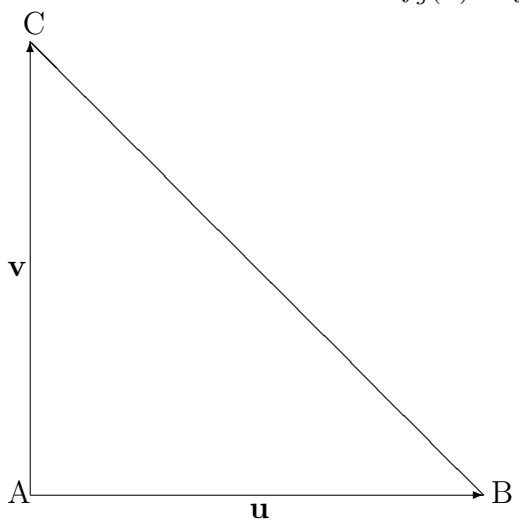

Figure 3.2: A Small Element

of $f(A)$, $f(B)$ and $f(C)$ only depend on the initialization. In other words, if the new triangle is $\Delta A'B'C'$ after the tramsform, then the following equations still hold

$$f(A') = \alpha, \quad f(B') = \beta, \quad f(C') = \gamma.$$

Define two vectors as

$$\mathbf{u} = (u_1, u_2) = \overrightarrow{AB} = (x_2 - x_1, y_2 - y_1) \tag{3.4}$$

$$\mathbf{v} = (v_1, v_2) = \overrightarrow{AC} = (x_3 - x_1, y_3 - y_1). \tag{3.5}$$

Denote the area of the triangle by S_Δ. Then we have

$$S_\Delta = \frac{1}{2}(u_1 v_2 - u_2 v_1) = \frac{1}{2}\mathbf{u} \cdot \mathbf{v}^\perp, \tag{3.6}$$

where

$$\mathbf{v}^\perp = (v_2, -v_1).$$

To compute the energy in the triangle, we should first find a linear function $L(x, y)$ in ΔABC such that

$$\begin{cases} L(A) = f(A) = \alpha \\ L(B) = f(B) = \beta \\ L(C) = f(C) = \gamma \end{cases} . \tag{3.7}$$

Furthermore, if $\mathbf{a} = (a_1, a_2)$ denotes the gradient of L, then $\mathbf{a}$ should satisfy

$$\mathbf{a} \cdot \mathbf{u} = \beta - \alpha, \quad \mathbf{a} \cdot \mathbf{v} = \gamma - \alpha. \tag{3.8}$$

By equation (3.8), we have

$$\begin{cases} a_1 u_1 + a_2 u_2 = \beta - \alpha \\ a_1 v_1 + a_2 v_2 = \beta - \gamma \end{cases} \tag{3.9}$$

The solution of the system (3.9) is

$$\begin{cases} a_1 = \dfrac{\begin{vmatrix} \beta-\alpha & u_2 \\ \gamma-\alpha & v_2 \end{vmatrix}}{\begin{vmatrix} u_1 & u_2 \\ v_1 & v_2 \end{vmatrix}} \\ a_2 = \dfrac{\begin{vmatrix} u_1 & \beta-\alpha \\ v_1 & \gamma-\alpha \end{vmatrix}}{\begin{vmatrix} u_1 & u_2 \\ v_1 & v_2 \end{vmatrix}} \end{cases} . \tag{3.10}$$

It is easy to find that the denominators of the solution are just the $2S_\Delta$. Since we can consider that $\nabla f_g = \nabla L$ in the small triangle ΔABC, we can use the following approximation to compute the magnetic energy in ΔABC

$$\begin{aligned} I_\Delta &= \tfrac{1}{2}\int_{\Delta_{ABC}} |\nabla f_g|^2 dx \\ &\approx \tfrac{1}{2}\int_{\Delta_{ABC}} |\nabla L|^2 dx \\ &\approx \tfrac{1}{2}(a_1^2 + a_2^2) S_\Delta \,. \end{aligned} \tag{3.11}$$

For the energy of density change, assume the area changes little after the transform $g \in$SDiff(M). So we have

$$\Big|\frac{\partial g(x)}{\partial x}\Big| \approx \frac{S_\Delta}{S_0} \tag{3.12}$$

where S_0 is the initial area. Then we can compute the energy of density change in the small triangle

$$F_\Delta = \int_{\Delta_{ABC}} P\Big(\Big|\frac{\partial g(x)}{\partial x}\Big|\Big) dx = P\Big(\frac{S_\Delta}{S_0}\Big) S_0. \tag{3.13}$$

By equation (3.11) and (3.13) we know the total energy in ΔABC is approximated

by

$$\begin{aligned} E_\Delta &= I_\Delta + \lambda F_\Delta \\ &= \tfrac{1}{2}(a_1^2 + a_2^2) S_\Delta + \lambda P\Big(\tfrac{S_\Delta}{S_0}\Big) S_0 \end{aligned} \tag{3.14}$$

To obtain the energy in the domain M, we should compute the energy in each element and add them together: $E = \sum_i E_{\Delta_i}$.

Thus, the energy E is a function of the coordinates of the vertices of the triangles Δ_i'. Its minimization is done by the gradient method.

The domain M is a rectangle $0 < x < a, \quad 0 < y < b$. It is divided into equal squares $R_{m,n} : \quad ml < x < (M+1)l, \quad nl < y < (n+1)l$ where l is a square size. Each square $R_{m,n}$ is divided by a diagonal into two triangles, $\Delta^+_{m,n}$ and $\Delta^-_{m,n}$. These triangles are the finite elements we use in our solution.

Consider the minimization of the energy. Suppose $Q(x_i, y_i)$ is a common vertex of several small triangles, as shown in figure 3.3. To minimize the functional U we

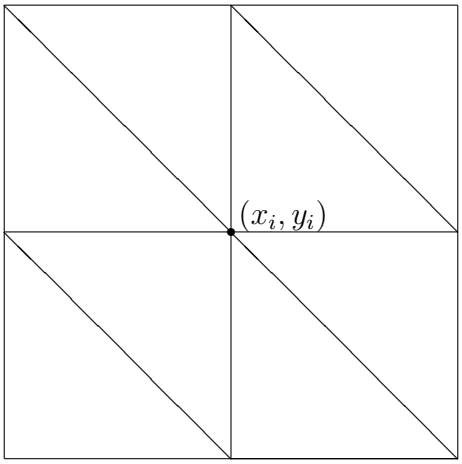

Figure 3.3: A Common Vertex of several small triangles

should only move Q along the opposite direction of the gradient $(\frac{\partial U}{\partial x_i}, \frac{\partial U}{\partial y_i})$. To find the gradient numerically we replace the partial derivatives by finite differences:

$$\begin{aligned} \frac{\partial U}{\partial x_i} &\approx \frac{U(x_i + \delta, y_i) - U(x_i, y_i)}{\delta} \\ \frac{\partial U}{\partial y_i} &\approx \frac{U(x_i, y_i + \delta) - Uy(x_i, y_i)}{\delta} \end{aligned}$$

where δ is a very small positive number, such as 10^{-9}. Then the new position $Q'(x_i', y_i')$ is

$$(x_i', y_i') = (x_i, y_i) - h(\frac{\partial U}{\partial x_i}, \frac{\partial U}{\partial y_i}) \tag{3.15}$$

where h is the step size. By this method, we can relocate every point on the grid of the finite element method to minimize the energy.

In the actual computation of partial derivatives of U, there is no need to compute the full energy change resulting from the small variation of the vertex position. Let us call the star of the vertex Q, $St(Q)$, the union of all triangles having Q as a vertex. Then the change of position of Q changes the contributions of the triangles in $St(Q)$ only. Thus, to find the partial derivatives of U with respect to the displacement of the vertex Q, we need to compute the contribution to the energy from the triangles in $St(Q)$ only.

The minimization proceeds as follows.

1. Divide the domain into small triangles.

2. Store the positions of vertices in the matrices Ax and Bx, respectively. Compute the value of f at each point and store in the matrix F.

3. Minimize the energy. For each step, compute the gradient and store them in the matrices ∂Ax and ∂Ay. We should note that the boundary points can only move along the boundary. Define the new matrices by

$$Ax = Ax - h\partial Ax \tag{3.16}$$

$$Ay = Ay - h\partial By. \tag{3.17}$$

The stepsize h is crucial in the minimization process. If h is too small, the minimization takes impractically long time. On the other hand, if h is too large, the process becomes unstable, and does not converge at all (it "explodes"). So, we should use *Adaptive Stepsize* (see appendix or [16]) to control h (which is not constant any

more, but is chosen at every step). To avoid the oscillation, the grid point moving forward and backward, we use the *Fast Fourier tramsform* (see appendix) to enhance the efficiency. Meanwhile, we record the total energy in the whole domain for each step.

4. Terminate the program when the total energies E_{new} for this step and E_{pre} satisfy

$$E_{pre} - E_{new} < \theta_t, \tag{3.18}$$

where θ_t is the given number to control the error.

Now suppose that the given function in **Problem 2** is $f = \sin(\frac{\pi}{2}(x+4y))\sin(\frac{\pi}{2}(x-4y))$ with the domain $M = [0,1] \times [0,0.25]$. This is a periodic function and the domain which we consider is a quarter of the period. Thus, we just minimize the Dirichlet energy having the same symmetry and the full doubly periodic solution can be obtained by reflections.

We first divide the domain into some small squares with side length $1/N$ (say N=128) and then divide the each square into two triangles as shown in figure 3.3.

Then the initial area of each triangle is $1/(2N^2)$. Then we initialize the matrix Ax, Ay. Meanwhile, we compute the function's values at corresponding grid-point and use F to record them. The following graph shows the level lines of the function f in the domain.

After the initialization, we can minimize the energy. Here we use the function

$$P(t) = t + \frac{1}{t} - 2, \quad t \in (0, +\infty) \tag{3.19}$$

to compute the energy of density change. We found experimentally that $\lambda = 100$ is a suitable value for this problem.

Figure 3.6 shows the grid after the minimization (every cell is a union of two

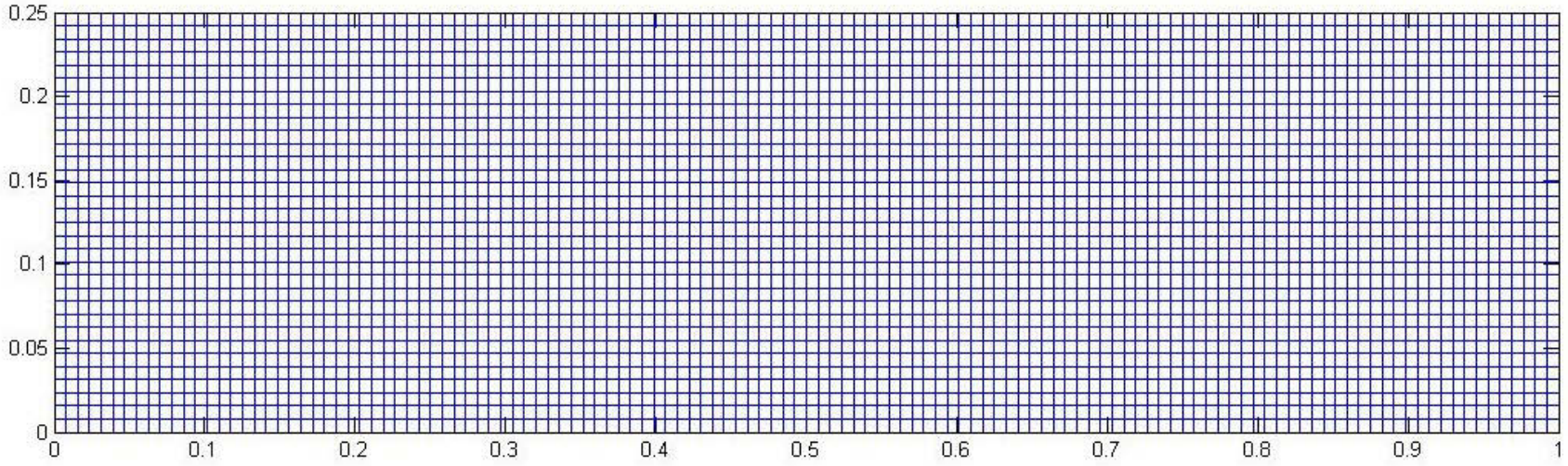

Figure 3.4: The Division of the Domain

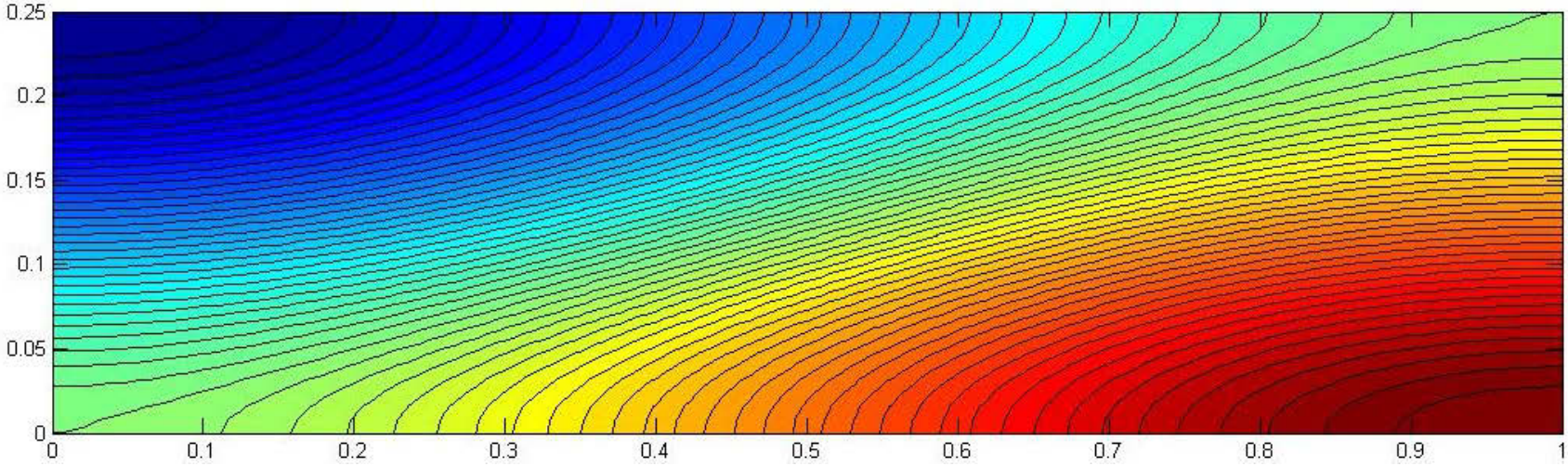

Figure 3.5: The Initial Level Lines

triangles; diagonals are not shown for better view). Compare with figure 3.4 it is obvious that the elements (small squares) near the diagonal (from the top right corner to bottom left corner) are severely skewed. Especially, the elements close to the right top and left bottom shift to the opposite side and are squeezed to be quite long and narrow. This means that the transformation g delivering a minimum to the energy is no longer smooth; it is discontinuous along the diagonal. This is clear from figure 3.7 which contains the level lines of the displacement.

We should note that although the minimizer function is not continuous along the diagonal, the discontinuity will not result in infinite energy since the function is constant on the diagonal.

As mentioned before, the given function is a periodic function, so we can get a whole period by reflections (see figure 3.8 and 3.9).

From those two figures, we can find that the saddle point $(0, 0)$ is replaced by a segment, which implies an existing singularity. Thus, there is a X-Y transition in this example.

3.2 Water Bag Method

The Finite Element Method has an obvious advantage of universality: it is applicable to arbitrary domains and functions f. On the other hand, it has a built-in disadvantage. Namely, it is difficult to construct piecewise-linear transformations which are area-preserving, i.e. such that the area of any triangle Δ_i' is equal to the area of corresponding triangle Δ_i. The number of conditions is very close to the number of free parameters, and as a result, we cannot find such transformation close to a given smooth diffeomorphism. We have to admit some distortion of areas, which is taken into account by the compression term in the energy. Therefore, the solution is not very accurate, and to decrease the error, we have to decrease the size of triangles,

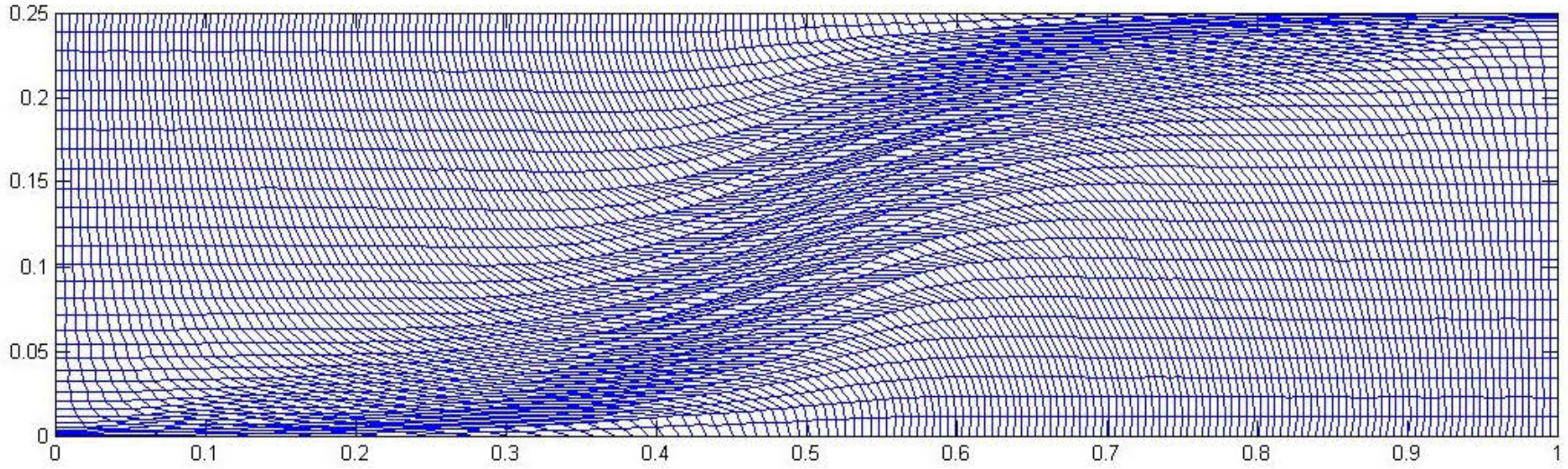

Figure 3.6: The Grid after Minimization

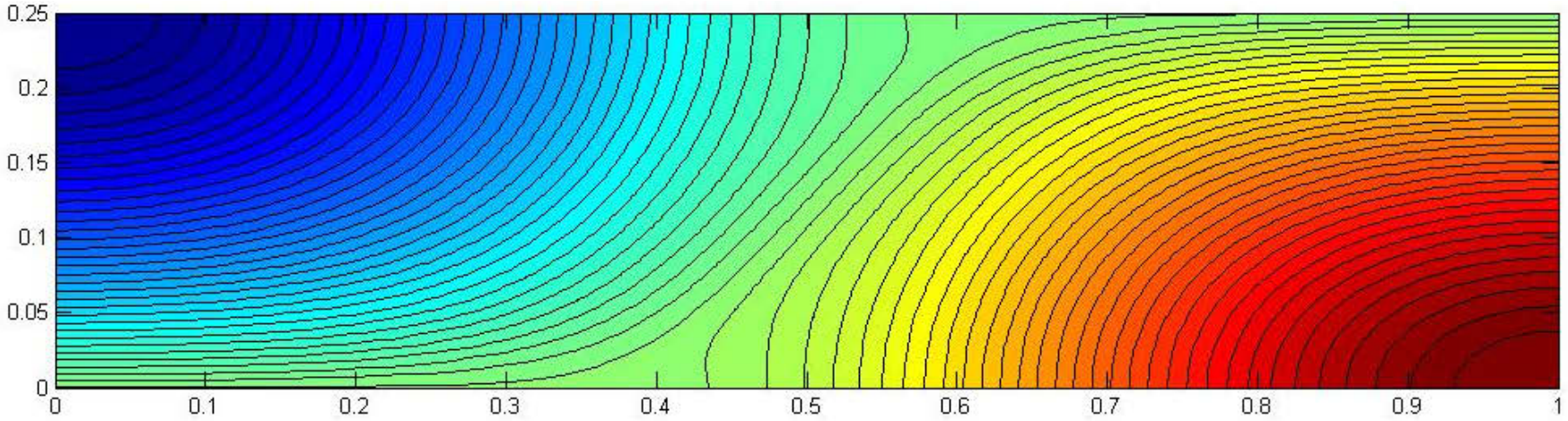

Figure 3.7: The Level Lines of the Minimizer Function

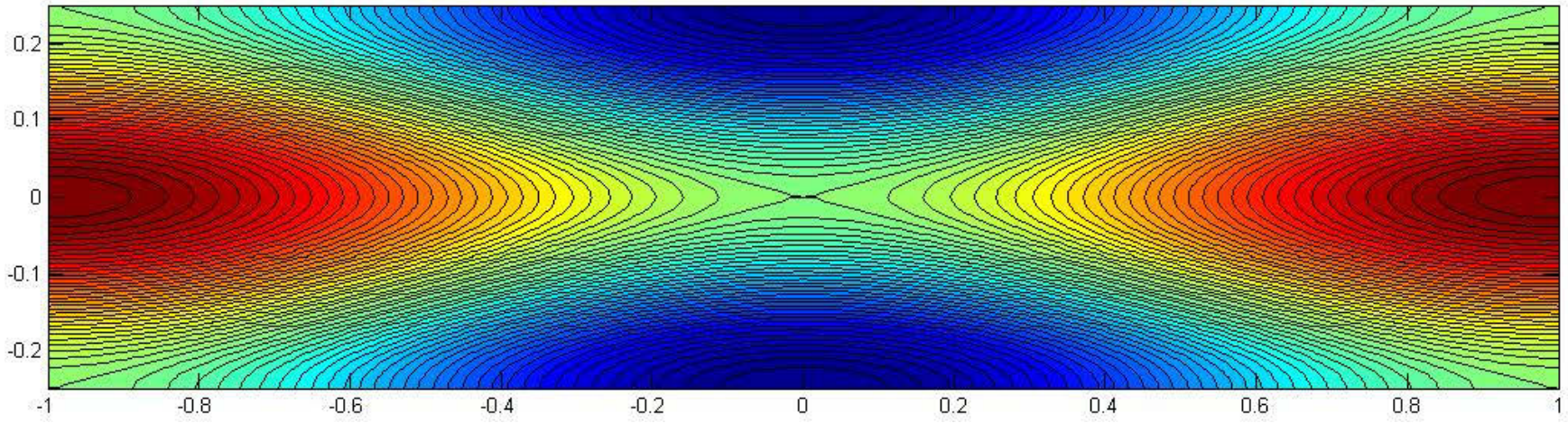

Figure 3.8: The Level Lines of the Minimizer Function

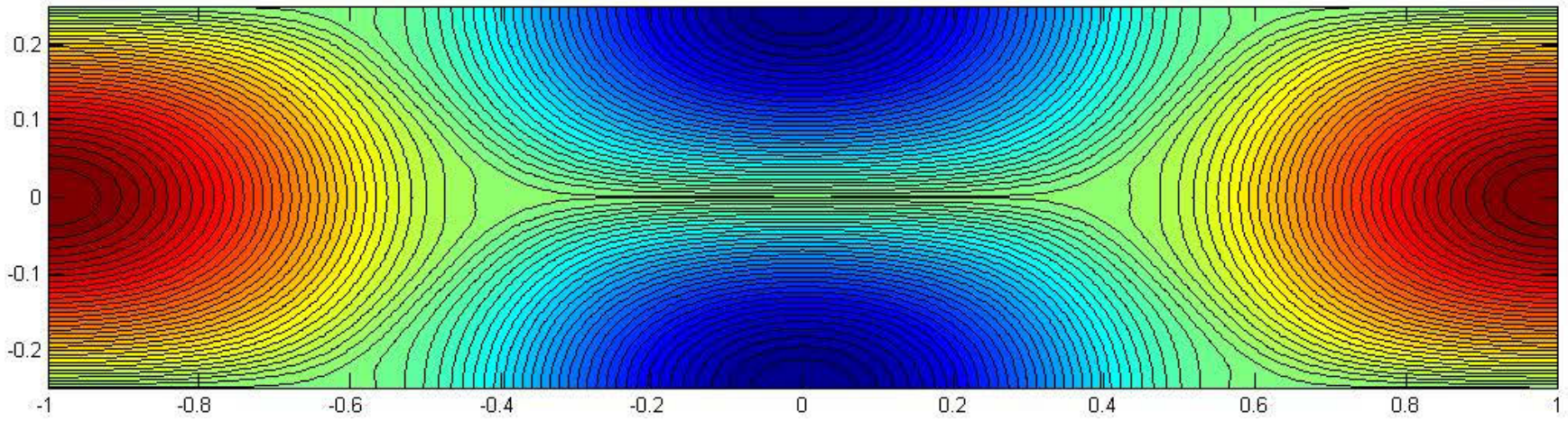

Figure 3.9: The Level Lines of the Minimizer Function

thus increasing the computation time.

It is quite natural to use the level lines of the function f as a basis for the partition of the domain M. This is the idea of the Water Bag Method.

To solve Problem 2 numerically we should always keep in mind that the transformation g must preserve areas. In last method, we employ the energy of density changes as the penalty function to preserve the areas of each elements. However, the "areas" to be preserved are bounded by the level lines.

In this method, we will use the differences between the areas after the transformation and the original areas as the penalty function. The areas bounded by the level lines will be computed at every step, instead of considering the area of each elements in the FEM. So the result will be more accurate. And the displacement of the level lines can be observed directly during the process of the simulation.

To realize the water bag method, we should first plot some level lines of the given function f (the accuracy also depends on the number of level lines). Then select some points on each level line (uniform distances are not required, but the number of the points one each level line should be equal). We can divide the strip between two adjacent level lines into some small quadrilaterals (like FEM) by using those points on the level lines, as shown in figure 3.10.

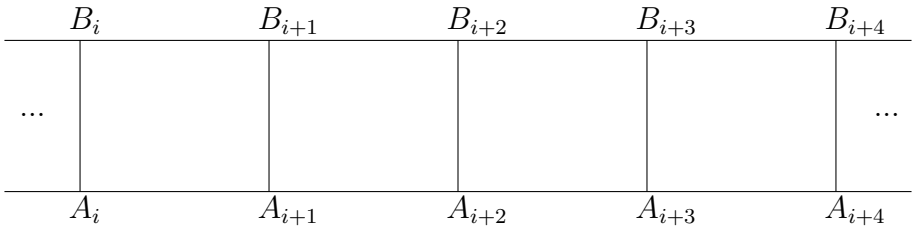

Figure 3.10: The Strip between Two Level Lines

For each quadrilateral, we can divid into two triangles (see figure 3.11) and then compute the Dirichlet energy in the small triangle numerically by the method used in FEM. And we also use the same method in FEM for the minimization problem.

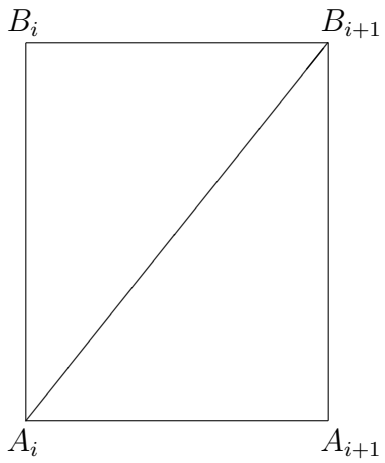

Figure 3.11: Division of Quadrilateral

Here we only take the magnetic energy into account, so we just minimize the Dirichlet energy. However, we should also check the areas as mentioned above for each step. In another word, if the current area is smaller than the initial area, we should expand to area bounded by the level line; otherwise, we should compress the area. Here we should note that distinct step sizes should be allocated for the two sub-steps to guarantee that the program works efficiently. Moreover, the ratio of the two step sized cannot be fixed. At the beginning, we can set the step size for the minimization larger to emphasize the energy part and, after running the algorithm for a while, we can decrease this step size to make sure the areas change little. Thus, one of the critical point of the simulation is to keep the balance of the two step sizes.

We give a brief description of the water bag method:

1. According to the given function f, define some level lines and select some points on the level line. The number of points on each level lined should be equal. Use the points to divid the strip between adjacent level lines.

2. Minimize the energy. For each step there are two sub-steps. One is to minimize the magnetic energy and the other is to check the areas bounded by the level lines. The steps sizes should be adjusted to make the program running well.

3. Terminate the program when the magnetic energy does not to change (de-

crease) anymore, and the differences between the current areas and the initial areas are smaller than the tolerant error.

First, let us consider a simple example of a doubly-connected domain. In our case, the domain is a square with a round hole. The function is 1 on the exterior boundary and 0 on the interior boundary. There are $N-2$ level lines between the boundaries. Suppose that the interior boundary is the first level line and the exterior boundary is the N-th level line. Then we define the f_i and λ_i, the function value of the i-th level line and the area bounded by the i-th level line and the interior boundary, by

$$f_i = \frac{i-1}{N-i} \tag{3.20}$$

$$\lambda_i = S_0 + \frac{i-1}{N-i}(S_N - S_0) \tag{3.21}$$

where S_0 and S_N are the areas of the round hole and the square, respectively, and $i = 1, 2, \ldots N$. At the beginning, we define all the level lines to be contours of a square, like the exterior boundary. The grid points are the intersection points of the level lines and the segments connecting the two boundaries. Furthermore, the grid points are restricted to move along the segments. Then we minimize the Dirichlet integral of this function by the method above. Figure 3.12 shows the configurations of the level lines of the minimizer.

It is observed that the configurations of the level lines are more like to the boundary which they are closer to.

Now consider a more complicated example. Suppose that a function f defined in the domain $[0,1] \times [0,1]$ has the minimum 0 at $(0,0)$ and the maximum 2 at $(1,1)$ (example: $f(x,y) = 1 - \cos(\frac{\pi}{2}(x+y))$. In this case, like in the previous one, we can anticipate the X-Y transition (and it really occurs). Therefore we have to introduce a grid which permits the Y-topology. Since we focus on the rearrangement of the minimizer, the initial configuration can be ignored. We want to define the position

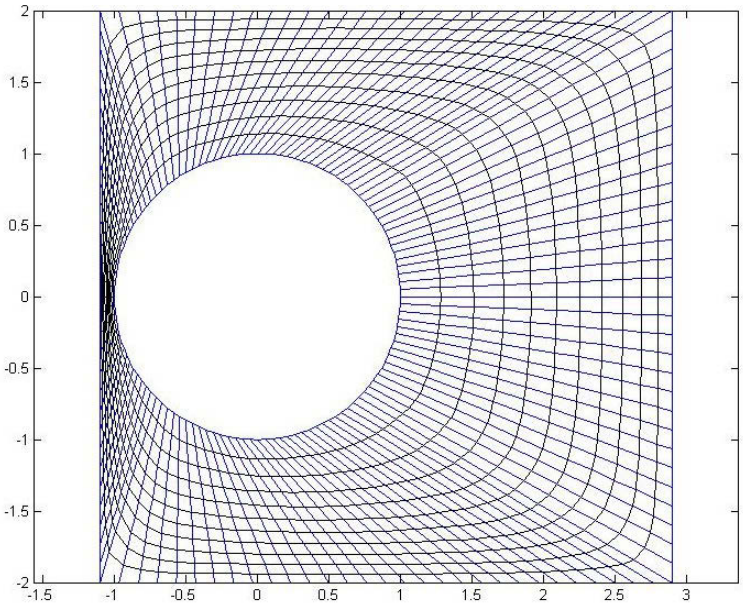

Figure 3.12: The Minimizer for a Function in a Domain with a Round Hole

functions of the grid points with respect to the value the given function f. We also employ another variable t to define the grid point. For convenience, we divide the domain into four parts.

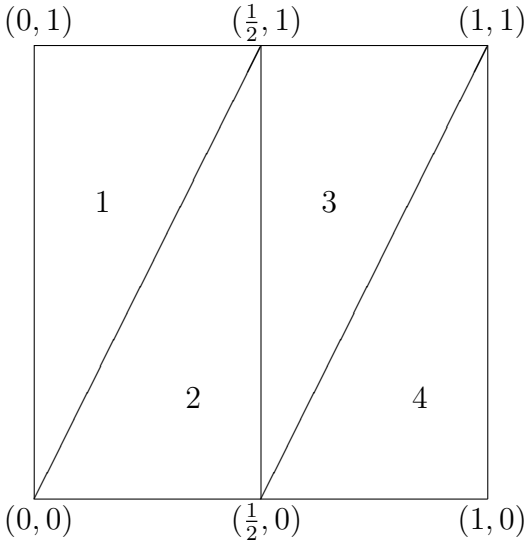

Figure 3.13: Partition of the Domain

Suppose that s is a value in the range of f, $[1,2]$ and $t \in [0,3]$. Let (x,y) be in the domain and define the initial position of the grid point by, see Figure 3.13,

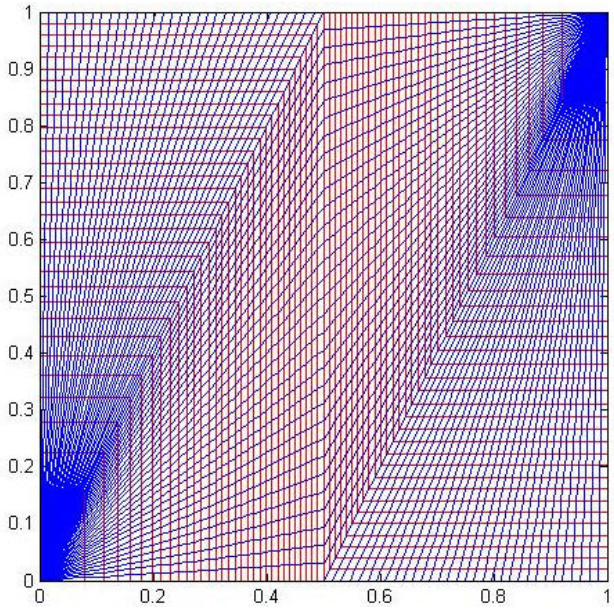

Figure 3.14: The Grid Points

if (x, y) in the area 1:

$$x(s,t) = \frac{1}{2}s \cdot t, \quad y(s,t) = s \tag{3.22}$$

if (x, y) in the area 2:

$$x(s,t) = \frac{1}{2}s, \quad y(s,t) = (2-t) \cdot s \tag{3.23}$$

if (x, y) in the area 3:

$$x(s,t) = \frac{1}{2}s, \quad y(s,t) = 1 - (2-s) \cdot (t-1) \tag{3.24}$$

if (x, y) in the area 4:

$$x(s,t) = \frac{1}{2}(2 - (2-s) \cdot (3-t)), \quad y(s,t) = s - 1. \tag{3.25}$$

Figure 3.14 shows the initial grid points. We can find that the method to define the grid points is similar to the polar coordinates. There are two distinct centers in the

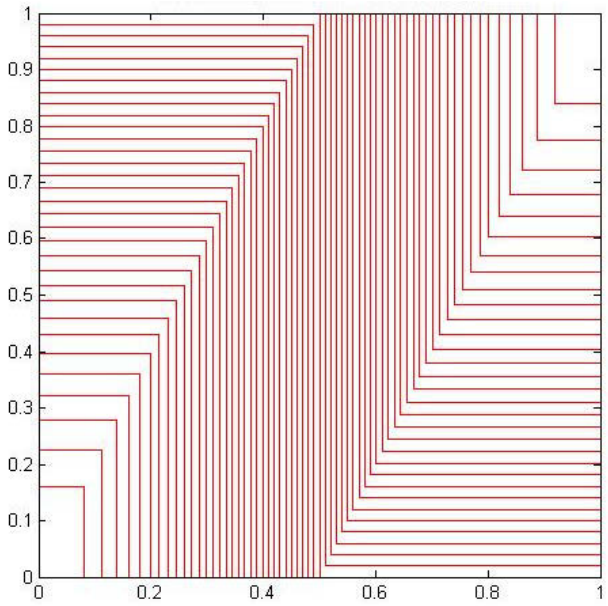

Figure 3.15: The Level Line

domain. The point $(0, 0)$ is the center of area 1 and 2 and the point $(1, 1)$ is the center of area 3 and 4. Paths (blue lines) radiate from these two points. In the functions $x(s, t)$ and $y(s, t)$ t defines the path and s defines the distance to the center.

Now, we choose the initial function f as a piecewise-constant function; its "level lines" are shown in the next figure (see figure 3.15). We should note that these are not the real level lines of the function f and we just minimize the energy from this situation.

We should find an efficient way to record the x and y for the numerical computation. If we use X and Y as the matrices to record the coordinates x and y, respectively, then X and Y should have the form from figure 3.16. The parts 1, 2, 3 and 4 are corresponding the areas in figure 3.13. In other words, the part 1 stores the coordinate of points in area 1. Furthermore, all the entries in the blank part of figure 3.16 are 0. We should also construct the matrices S and T for s and t with the same form as X and Y (see figure 3.17).

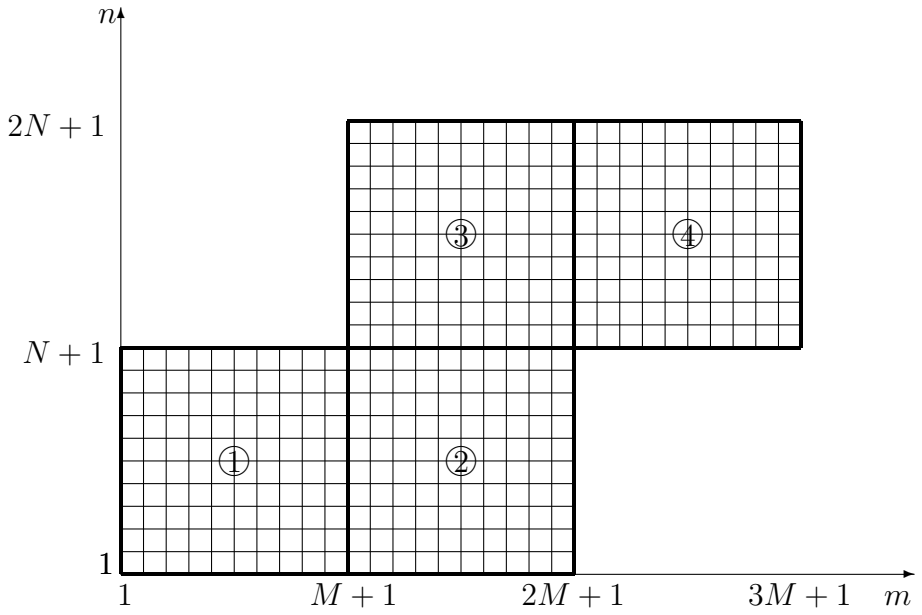

Figure 3.16: The Form of Matrices which Store the Coordinates

We initialize the matrices S and T as

$$S(n,m) = (n-1)/N \tag{3.26}$$

$$T(n,m) = (m-1)/M \tag{3.27}$$

where m and n satisfy

$$1 \le n \le N+1, \quad 1 \le m \le 2M+1 \tag{3.28}$$

or

$$N+1 \le n \le 2N+1, \quad M+1 \le m \le 3M+1. \tag{3.29}$$

The rest of the entries in the matrices are set as 0. By the definition of x and y, we initialize X and Y as

$$X(n,m) = x(S(n,m), T(n,m)) \tag{3.30}$$

$$Y(n,m) = y(S(n,m), T(n,m)). \tag{3.31}$$

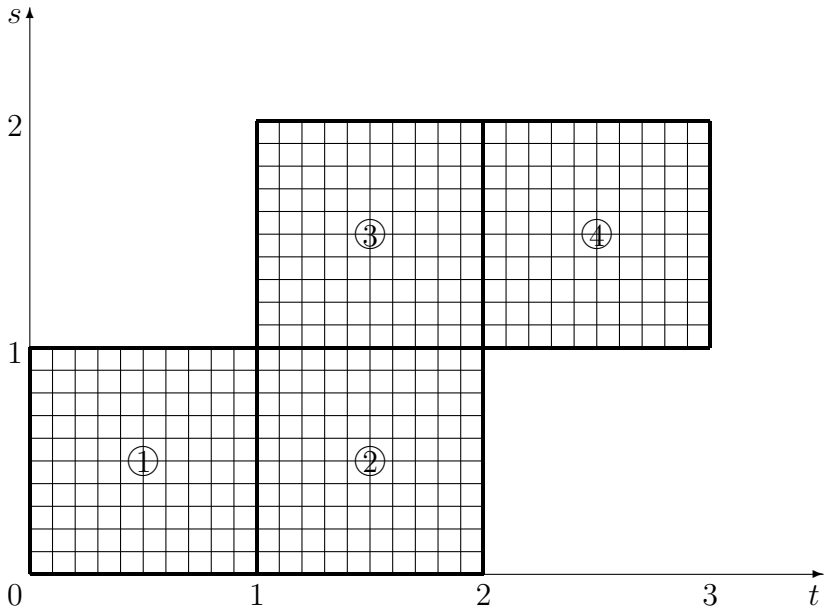

Figure 3.17: The Form of Matrices S and T

Since the path which a certain point is on depends on the variable t, the matrix T will not be changed during the progress of minimization. We change the matrix S, namely, the distances of grid points to the centers, to minimize the energy. We use the similar method in the first example. The only difference is that we we consider the magnetic energy as function with respect to s in this case. Thus, we will first change $S(n,m)$ a little, say $S(n,m)+\delta$, and get the new value of $X(n,m)$ and $Y(n,m)$ by (3.30) and (3.31). Then find the change of energy in a neighborhood of $(X(n,m),Y(n,m))$. In this way, we can compute the derivative $\partial S(n,m)$ numerically. To minimize the energy, the new matrix is

$$S_{new} = S_{current} - h \cdot \partial S \tag{3.32}$$

where h is the step size.

But it is not sufficient if we only optimize S. We expect the grid points to have more freedom. Thus, we use another transformation G_α defined by

$$G_\alpha(x,y) = (\alpha(x(1-x)(y-0.5)) + x, y) \tag{3.33}$$

where (x,y) is a grid point and α is an unknown variable. This transformation allows

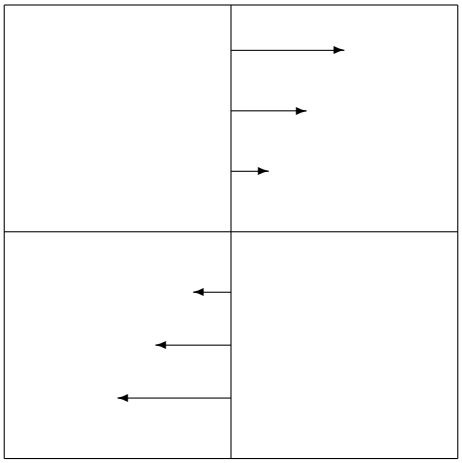

Figure 3.18: The G_α Transformation

the grid points to move horizontally. Figure 3.18 show the situation of $\alpha < 0$. So the paths which radiate from the center will bend and their curvatures depend on α. When we take the transformation for the matrices X and Y, we can get the new positions of grid points. In this case, the magnetic energy in the domain is a function with respect to α. Thus, we can first define a initial value of α and then optimize α by computing the derivative $\partial\alpha$ numerically. Define the new α by

$$\alpha_{new} = \alpha_{current} - \eta \cdot \partial\alpha \tag{3.34}$$

where η is the step size.

The parameter α is very crucial to check whether there is $X-Y$ transition. When the absolute value of α is large enough, the end points of the vertical line (between $(\frac{1}{2}, 0)$ and $(\frac{1}{2}, 1)$) can reach the vertices of the square, say, $(0, 1)$ and $(1, 0)$. In this case, there is no singular line in the minimizer.

We should note that these two transformations can not be taken in the same time. In other words, if we want to compute the matrix ∂S, we should save the X and Y from the previous step and then optimize α by using the X and Y from the previous step, instead of the current step X and Y which are defined by the new matrix S.

After finding the new S and α, we can compute the new X and Y.

Let us consider preserving the areas. Since each row in X and Y record the grid points on the same level line, it is quite convenient to compute the area bounded by the level line. When we initialize the matrices X and Y, we should use a column vector λ^0 to store the areas by the level lines as well. We should check the areas and record in a column vector λ each step when we minimize the magnetic energy by changing S and α. Since the S decides the distance between the grid points and the center, we should adjust the values of S to preserve the area. For example, if $\lambda_i < \lambda_i^0$, then we change $S(i,j)$ by the following formula

$$S(i,j) = S(i,j) + \epsilon(\lambda_i^0 - \lambda) \tag{3.35}$$

where $1 \leq j \leq 2N+1$ or $M+1 \leq j \leq 3M+1$ and ϵ is the given step size.

For the different step size (h, η and ϵ) we should keep a balance among them to make the program run efficient. At first we can set h and η a little larger to make the energy reach the minimum faster. And then ϵ can be set larger to guarantee preserving the areas.

Figure 3.19 is the rearrangement of the function after minimization. From the figure we can find the straight level line in figure 3.14 become the curved lines. Additionally, the vertical line (between $(\frac{1}{2}, 0)$ and $(\frac{1}{2}, 1)$) looks like the letter S and the end points do not reach the vertices of the square. Thus, there is $X-Y$ transition during the minimization. In other words, there is a singular line in the minimization function and the gradient is not continuous.

Actually, we can consider that this is the minimizer of the function similar to

$$f(x,y) = \sin(\frac{\pi}{2}(x+y))\sin(\frac{\pi}{2}(x-y)). \tag{3.36}$$

So figure 3.19 is just a piece of a whole period and we can expand the figure by

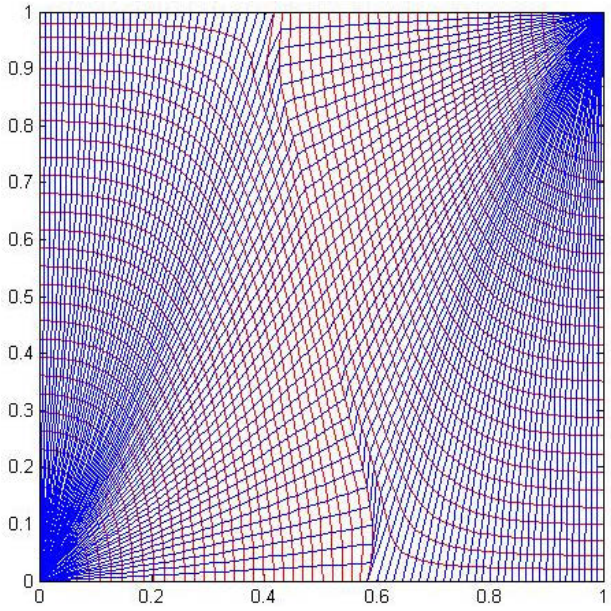

Figure 3.19: The Configuration of the Minimizer

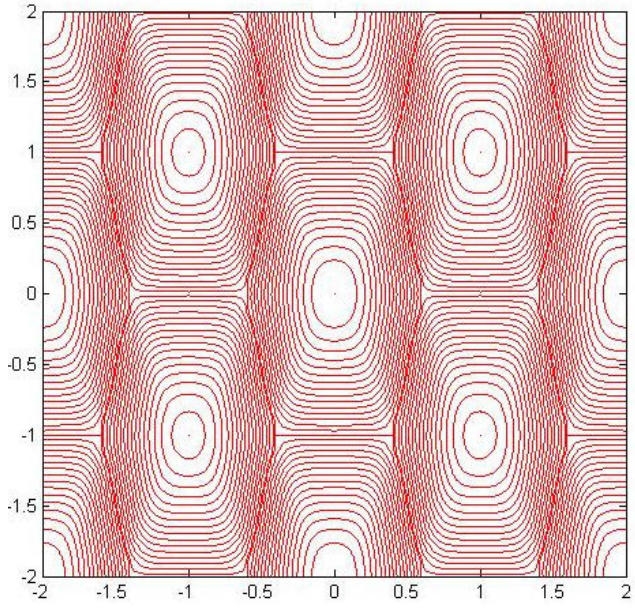

Figure 3.20: The Expansion of the Minimizer by Reflection

reflection as in the method of example 1. We obtain figure 3.20 and the singular lines are very obvious in this figure.

3.3 Level Lines in Bubbles

In the previous two examples we considered a periodic function on just a quarter of a period, instead of a whole period. Now we will try to simulate Problem 2 in a bounded domain (unit square) directly. We will use a different method which we call "the bubble method". Suppose the initial function f has the following property: the domain M can be divided into a finite number of domains M_i such that (1) the function f is constant on ∂M_i for all i; (2) The function f has a local maximum or minimum at some point $x_i \in M_i$ and no other critical points in every domain M_i (so that the saddle points of f belong all to $\bigcup_i \partial M_i$). In this case, we can find many piecewise-smooth area preserving maps $g : M \to M$ disconnected along $\bigcup_i \partial M_i$ such that $f_g = f \circ g^{-1}$ is continuous, and $\int_M |\nabla f_g|^2 dx < \infty$ (in fact ∇f_g is disconnected along $g(\bigcup_i \partial M_i)$. The weak solution of the magnetic energy minimizing problem should be looked for in the class just described. This was the case in the examples considered above.

We can regard the domains M_i as "slippery bubbles" with a fixed volume. The frozen magnetic field (or its stream function f) provides these bubbles with a sort of elasticity, and the bubbles are looking for an equilibrium, i.e. a configuration with a minimal potential energy. It should be stressed that the topology of the equilibrium configuration, i.e. which domains are touching each other and in which order, is not fixed; it should be found in the course of the solution.

Before solving Problem 2, let us consider a model problem, namely the problem of configuration of a collection of true bubbles (a "foam"). In this case, the energy is proportional to the length of $\bigcup_i \partial M_i$ (this means the sum of lengths of all simple

arcs comprising $\bigcup_i \partial M_i$, including the outer boundary ∂M). So, we are solving the following problem:

Problem 3. *Find the configurations of several bubbles in a unit square domain such that*

1. *the sum of areas is equal to the area of the domain;*
2. *the sum of perimeters is the smallest.*

We will consider the problem starting from the simplest condition, merely one bubble in the domain. It is obvious that the configuration of the bubble should be the same as the domain, namely, the unite square. But one wonders how to obtain the result numerically. In this case, we can set an initial configuration of the bubble, say a circle (see figure 3.21). Then we expect to inflate the bubble by some rules

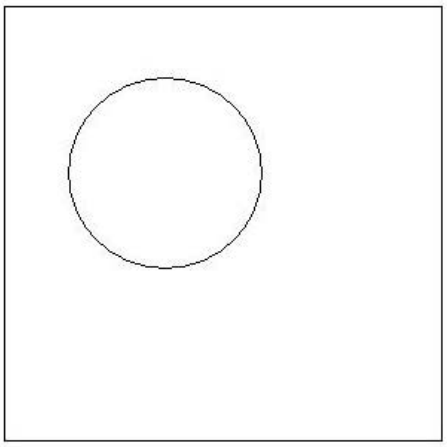

Figure 3.21: The Initial Configuration of One Bubble

such that we can obtain the correct configuration finally. To solve Problem 3, we should do two things: one is to make the value of bubble very close to the area of the domain; the other is to minimize the perimeters. However, if we want to solve the problem numerically, we should consider some other things. This is because it is possible that the bubble has been out of the range of the domain before it reaches the area of the domain (see figure 3.22). Thus, we have to add some restrictions for

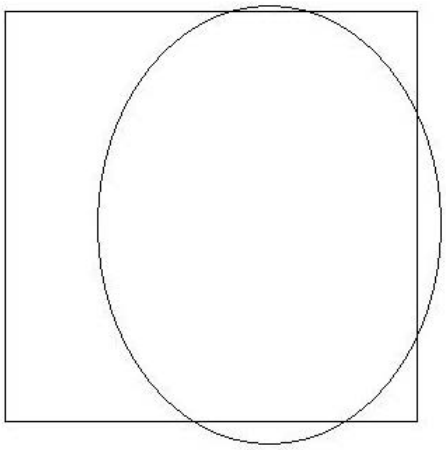

Figure 3.22: The Initial Configuration of One Bubble

the problem such that the bubble can "feel" the boundary of the domain. Here we will employ a functional, which is called the *potential energy*, as the restriction.

Definition 8. *Suppose* (x_f, y_f) *is a fixed point and* (x, y) *is any other point. We define the potential energy to the fixed point as*

$$d(x, y; x_f, y_f) = \frac{1}{(x - x_f)^2 + (y - y_f)^2} \tag{3.37}$$

It is obvious that the potential energy is just the reciprocal of the square of the distance between (x_f, y_f) and (x, y). So the energy will be very large if (x, y) is very close to (x_f, y_f). In the situation of problem 3, we can assume the fixed point is on the boundary of the domain and the (x, y) is a point on the bubble. Then the potential energy can be utilized to control the distance between the domain and the bubble. Since the point (x_f, y_f) is fixed, then d is a function with respect to (x, y) and the gradient of (3.37) is

$$u(x, y; x_f, y_f) = \operatorname{grad} d(x, y; x_f, y_f) = -\frac{2(x - x_f, y - y_f)}{((x - x_f)^2 + (y - y_f)^2)^2} \tag{3.38}$$

In fact, we should select a large number of points, say N, on the boundary, and the bubble during the simulation. Suppose $\{(x_f^i, y_f^i), 1 \leq i \leq N\}$ is the collection of the

points on the boundary. Then the potential energy to the boundary is

$$\begin{aligned} D(x,y) &= \sum_{i=1}^{N} d(x,y;x_f^i,y_f^i) \\ &= \sum_{i=1}^{N} \frac{1}{(x-x_f^i)^2+(y-y_f^i)^2} \end{aligned}$$

It follows the gradient of D is

$$\begin{aligned} U(x,y) &= \operatorname{grad} D(x,y) \\ &= \sum_{i=1}^{N} \operatorname{grad} d(x,y;x_f^i,y_f^i) \\ &= \sum_{i=1}^{N} -\frac{2(x-x_f,y-y_f)}{((x-x_f^i)^2+(y-y_f^i)^2)^2} \end{aligned}$$

We should keep the potential energy from being too large in order to avoid the point (x,y) too close to the boundary. Namely, the potential energy should be minimized when we adjust the area and perimeter of the bubble. To minimize the energy, we should define the new position of (x,y) as

$$(x,y)_{new} = (x,y)_{current} - h_1 \cdot U(x,y) \tag{3.39}$$

where h_1 is the step size.

Here we use matlab to simulate problem 3. Since the matrix operation is more efficient than the loop computation in matlab, we choose the matrix operation to compute the gradient. Suppose that the column vectors X and Y record the coordinates of the points on the bubble

$$X = (x_1, x_2, \cdots, x_{N-1}, x_N)^T \tag{3.40}$$

$$Y = (y_1, y_2, \cdots, y_{N-1}, y_N)^T, \tag{3.41}$$

where (x_i, y_i) and (x_{i+1}, y_{i+1}) are adjacent points. Similarly, the matrices X_f and Y_f record the coordinates of the points on the boundary

$$X_f = (x_f^1, x_f^2, \cdots, x_f^{M-1}, x_f^M)^T \tag{3.42}$$

$$Y_f = (y_f^1 1, y_f^2, \cdots, y_f^{M-1}, y_f^M)^T. \tag{3.43}$$

Then define the matrices A, B, C and D as

$$A = X \times J_{1,M} \tag{3.44}$$

$$A_f = J_{N,1} \times X_f \tag{3.45}$$

$$B = Y \times J_{1,M} \tag{3.46}$$

$$B_f = J_{N,1} \times Y_f \tag{3.47}$$

where $J_{m,n}$ is the $m \times n$ matrix of ones. Thus, all the above are $N \times M$ matrices. In matlab we can use the following code to compute the matrix C

```
C=((A-Af).^2+(B-Bf).^2).^2
```

Then the entry C_{ij} is $((x_i - x_f^j)^2 + (y_i - y_f^j)^2)^2$ and let

```
Ux=(A-Af)./C
```

```
Uy=(B-Bf)./C
```

where the entries Ux_{ij} and Uy_{ij} are $(x_i - x_f^j)/C_{ij}$ and $(x_i - x_f^j)/C_{ij}$. We can compute the new coordinates by using the code

```
X=X-h1*(sum(Ux))'
```

```
Y=Y-h1*(sum(Uy))'
```

where `sum(Ux)` treats the columns of Ux as vectors, returning a row vector of the sums of each column and `(sum(Ux))'` is the transpose of the matrix `sum(Ux)`, namely, a column vector.

That was the method to prevent the bubble getting out of the domain. Now let

us return to the problems of expanding the area and minimizing the perimeter. We also expect to expand the area by matrix operation. Suppose figure 3.23 is a piece of the bubble. We define the new position of the point (x_i, y_i) by the formula

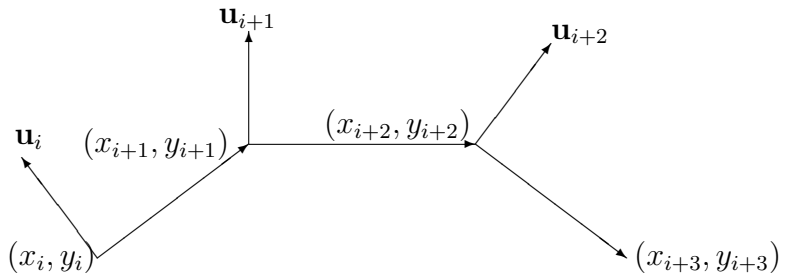

Figure 3.23: A Piece of the Bubble

$$(x_i, y_i)_{new} = (x_i, y_i)_{current} + h_2 \cdot (a - a_0) \cdot \mathbf{u}_{i+1} \tag{3.48}$$

where h_2 is the step size, a and a_0 are the current areas and the area of the fixed domain, respectively, and $\mathbf{u}_{i+1}$ denotes the vector

$$\begin{aligned} \mathbf{u}_i &= (x_{i+1} - x_i, y_{i+1} - y_i)^{\perp} \\ &= (-y_{i+1} + y_i, x_{i+1} - x_i). \end{aligned}$$

We should note that $\mathbf{u}_N = (-y_1 + y_N, x_1 - x_N)$. If we define matrix R as

$$\begin{pmatrix} -1 & 1 & 0 & \cdots & 0 \\ 0 & -1 & 1 & \cdots & 0 \\ \vdots & \ddots & \ddots & \ddots & \vdots \\ 0 & \cdots & 0 & -1 & 1 \\ 1 & 0 & \cdots & 0 & -1 \end{pmatrix} \tag{3.49}$$

then the i-th entries of $A \times X$ and $A \times Y$ are $x_{i+1} - x_i$ and $y_{i+1} - y_i$. By equation (3.48), we can use the following code to expand the area in matlab

```
X=X-h2*(a-a0)*(A*Y)

Y=Y+h2*(a-a0)*(A*X)
```

Meanwhile we should consider the current area a. We can use the following formula

$$a = \sum_{i=1}^{N-1}(x_{i+1} - x_i)(\frac{y_{i+1} + y_N}{2}) + (x_1 - x_N)(\frac{y_1 + y_N}{2}) \tag{3.50}$$

to compute the area bounded by a close curve numerically. Thus, we can compute a by matrix R

$$a = X^T \times R \times Y. \tag{3.51}$$

We use the matrix operation to minimize the perimeter as well. Figure 3.24 shows the method to minimize the perimeter. We define the vector $\mathbf{v}_i$ as

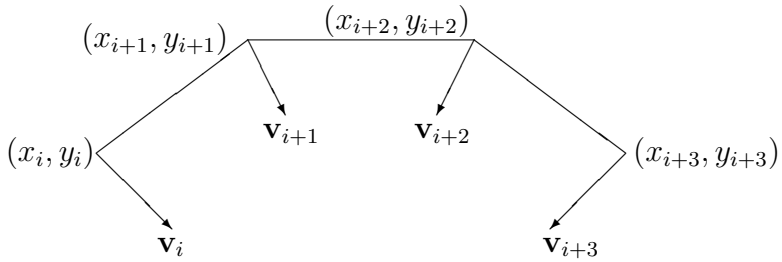

Figure 3.24: The Minimization of Perimeter

$$\mathbf{v}_i = h_3(x_{i-1} + x_{i+1} - 2x_i, y_{i-1} + y_{i+1} - 2y_i) \tag{3.52}$$

where h_3 is the step size.When $i = 1$ or N, we let

$$\mathbf{v}_1 = h_3(x_N + x_2 - 2x_1, y_N + y_2 - 2y_1) \tag{3.53}$$

$$\mathbf{v}_N = h_3(x_{N-1} + x_1 - 2x_N, y_{N-1} + y_1 - 2y_N). \tag{3.54}$$

For convenience, we use the matrix L

$$\begin{pmatrix} -2 & 1 & 0 & \cdots & 0 & 1 \\ 1 & -2 & 1 & 0 & \cdots & 0 \\ 0 & 1 & -2 & 1 & \cdots & 0 \\ \vdots & \ddots & \ddots & \ddots & \ddots & \vdots \\ 0 & \cdots & 0 & 1 & -2 & 1 \\ 1 & 0 & \cdots & 0 & 1 & -2 \end{pmatrix} \tag{3.55}$$

In this case, if we let

$$V_x = h_3 \cdot D \times X \tag{3.56}$$

$$V_y = h_3 \cdot D \times Y \tag{3.57}$$

then we can define the new coordinates in matrix form by

$$X_{new} = X_{current} + V_x \tag{3.58}$$

$$Y_{new} = Y_{current} + V_y. \tag{3.59}$$

Consequently, we should do three things for each step:

1. expanding the area
2. minimizing the perimeter
3. minimizing the potential energy

to solve Problem 3 numerically by running the program in matrix form. There are distinct step sizes (h_1, h_2, h_3) for each sub step. During the simulation, we can change the step size to keep the program running stable. For example, the step size (h_2) for the area should be larger than the others at the beginning and when the area is very close to the area of the domain, we should decrease the h_2 and increase the step size

(h_1) for the potential energy to guarantee the bubble in the domain.

Let the unit domain be $[-0.5, 0.5] \times [-0.5, 0.5]$. Figure 3.25 is the simulation result for one bubble. From the picture, we can find that the configuration of the bubble

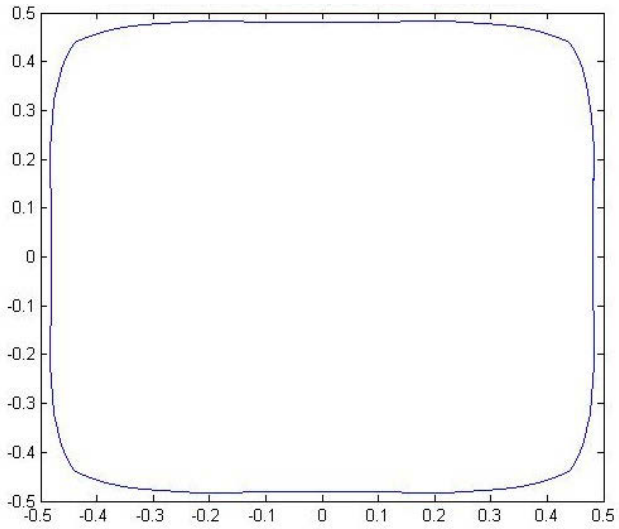

Figure 3.25: One Bubble in the Domain

is not the same as the domain. This is because there are potential energy between the bubble and the boundary of the domain. In spite of this, the configuration is still very close to the domain.

Now we can consider more bubbles. The methods of minimizing the perimeter and expanding the area are the same as one bubble. However, we should not only consider the potential energy between the boundary and the bubble, but also consider the potential energy between different bubbles. In this case X_f and Y_f should record the coordinates of the boundary of the other bubbles. Then we can use the same method to minimize the potential energy. In this case, the bubble areas are adjusted for each bubble separately; this means that the area term in the total energy is proportional to $\sum_i (a_i - a_i^0)^2$ where a_i are the current bubble areas, and a_i^0 are the prescribed ones (so that $\sum_i a_i^0 = 1$). Figure 3.26 and 3.27 are the configurations of the two and three bubbles, respectively.

This method works for arbitrarily many bubbles.

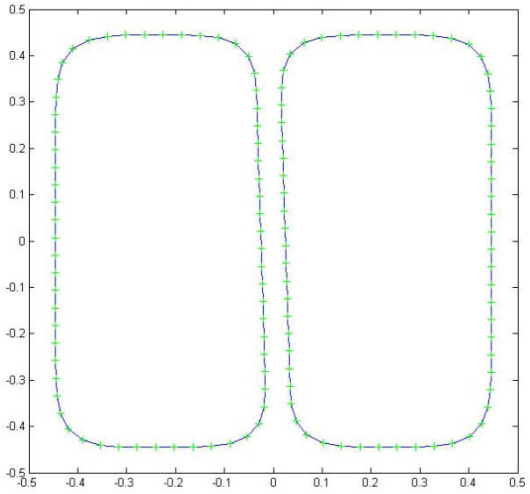

Figure 3.26: Two Bubbles in the Domain

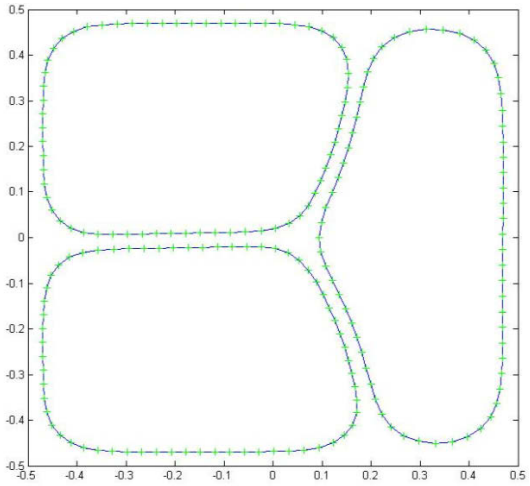

Figure 3.27: Three Bubbles in the Domain

We utilize the model of Problem 3 to solve Problem 2 numerically. Suppose that the function f has two maxima and two minima in the square domain (to be concrete, we consider the function $f(x, y) = \sin(2\pi x) \cdot \sin(2\pi y)$). In this situation, we can assume there are four bubbles in the domain. The function f has the maxima $f = 1$ at the centers of the top right bubble and bottom left bubble and has the minima $f = -1$ at the other two centers. On the boundaries of the bubbles $f = 0$. Furthermore, there are some intermediate level lines between the center and the boundary in each bubble. For numerical computation, we set the i-th level lines

with the value $f_i = \pm i/N$ where N is the number of level lines (including the center and the contour line) and $1 \leq i \leq N$. We expect that the area S_i bounded by the i-th level line is equal to a quarter of the area bounded by the level line of the function $\sin(\pi x)\sin(\pi y)$. So the area denoted by λ is a function with respect to f. We computed this function numerically; Figure 3.28 is the graph of $\lambda(f)$.

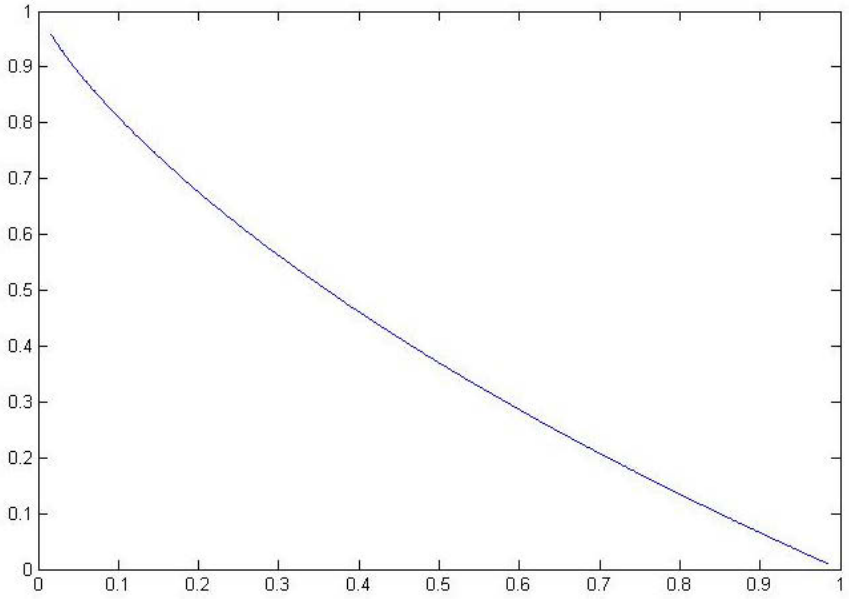

Figure 3.28: The Curve of $\lambda(f)$

Figure 3.29 shows the initial condition of the functional to be minnimized. We can consider each bubble as an individual domain and minimize the magnetic energy by the water bag method. However, the contour lines of the bubbles are level lines as well. We can change the configurations by the method in Problem 3. Thus, we adjust the configurations of the bubbles while the magnetic energy is minimized.

Moreover, we expect that the quadrangle elements between the level lines are very close to rectangles to increase the accuracy. Here we use the grid correction and phase correction. The grid correction is to make the points on level lines equidistant. Suppose (x^i_j, y^i_j) and $(x^i_{(j+1)}, y^i_{(j+1)})$ are two adjacent points. For grid correction we define the new position of $(x^i_{(j+1)}, y^i_{(j+1)})_{new}$, such that the vector from$(x^i_{(j+1)}, y^i_{(j+1)})$ to $(x^i_{(j+1)}, y^i_{(j+1)})_{new}$ having the same direction of the vector from $(x^i_{(j+1)}, y^i_{(j+1)})$ to

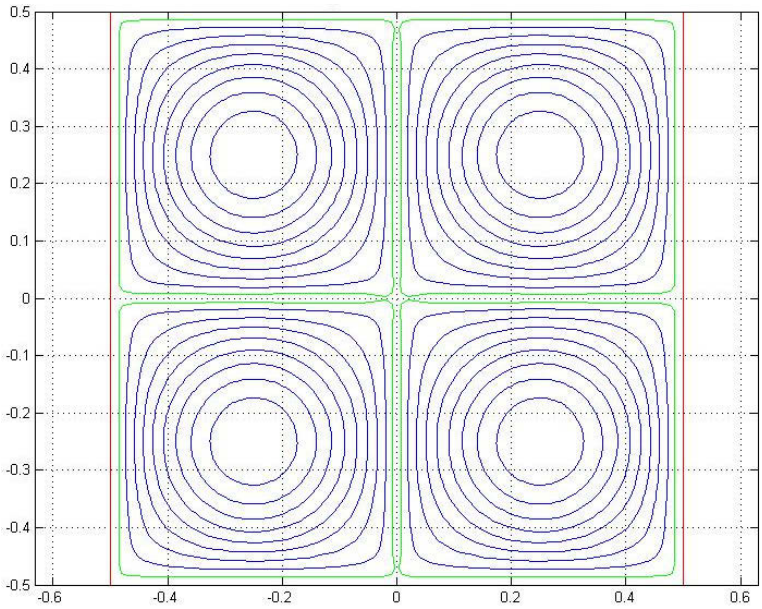

Figure 3.29: Four bubbles with Level Lines in the Domain

$(x^i_{(j+1)}, y^i_{(j+1)})$ and the length of the vector equals the Mth of length of the level line where M is the number of points on the level line. The phase correction can prevent the small elements skew very much. We redefine the indices of the points on the level lines. For example, (x^i_1, y^i_1) is the point on the i-th level line. We define the closet points on the $(i+1)$-th level line to (x^i_1, y^i_1) to be $(x^{(i+1)}_1, y^{(i+1)}_1$ and define the rest of the points in counterclockwise order. In this way, the small elements are always like rectangles.

Note that the initial configuration (Figure 3.29) is already an equilibrium (because the function $f(x, y) = \sin(2\pi x) \cdot \sin(2\pi y)$ is an eigenfunction of Laplacian, and hence a stream function of a steady solution of the Euler equations, for it satisfies (2.47). But this is not a local minimum of magnetic energy. Hence, we could use the method of the gradient descent, if we start from a different configuration which is close to the equilibrium, but lacks the symmetry. To do it, the initial configuration was chosen such that the position of a local maximum in one of the bubbles was randomly displaced, and then the minimization was started. The small asymmetry in the initial configuration grew up, and the result of minimization is shown at Figure 3.30. It is

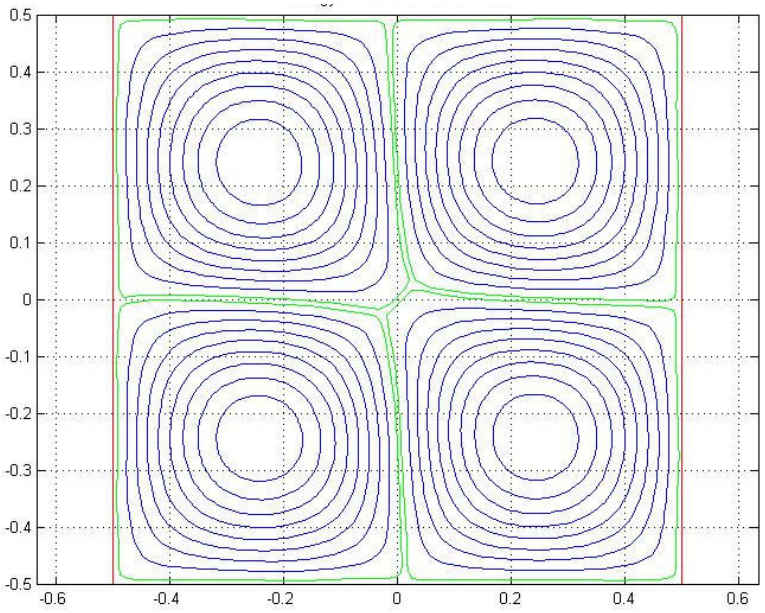

Figure 3.30: The Minimizer of Four bubbles with Level Lines

clearly seen that two opposite bubbles are touching one another along a segment ("a bridge"), while two other bubbles stay apart. So, this is a clear case of an X-Y transition, like in the examples considered before. Note that the bridge orientation is not unique; we could turn the picture by $\pi/2$, and get another minimizer with the same energy. To be sure, we found the value of the magnetic energy for the last configuration; it is (numerically) $E = 10.3826$, while for the initial (symmetric) configuration it was $E_0 = 11.2227$.

3.4 Methods Discussion

In this chapter we used three different methods to solve one problem. We used FEM first because it is very convenient to compute the Dirichlet integral numerically. But there are some disadvantages. First, when we compute the Dirichlet energy, the small elements (quadrangles) should be very close to rectangles. However, it is observed in Figure 3.6 that the elements on the diagonal are quite skewed. So the approximation is not too good in this case. Another disadvantage is that FEM cannot guarantee area-

preserving transformations. We just used the energy of density change to preserve the area of small elements. But, in fact, we cannot check the areas bounded by the level lines. To obtain a more accurate result, we used the water bag method.

The advantage of the water bag method is that we can observe the level lines during the transformation. We can check the areas inside each level line at each step to preserve them. Thus, the result is more accurate. And the result does not depend on the initial configurations. We should only define the values of the function and the areas bounded by the level lines initially. However, there is a disadvantage: to use this method, we should know in advance the topology of the minimizer, i.e. the configuration of its level lines and critical points. We need some grid (like a polar system of coordinates) to define the coordinates of grid points. But the grid points can only move along the paths defined at the beginning, so the lack of freedom affects our possibilities.

The last method, the bubble method, offers an opportunity to observe the singular line clearly. The "bridge" in Figure 3.30 is just the singular line. Although we employ the water bag method to minimize the energy, we can make the small elements more like rectangles. This is because we consider the whole level lines here, instead of pieces of them, and we can use the grid correction and phase correction to adjust the small elements. The disadvantage of this method is that there is a potential energy between the boundary and the bubbles. It results in some blank space between them. This is why the singular line looks like a narrow strip ("bridge") here.

Chapter 4

Conclusion

From Chapter 2, we know that the problem of minimization of the Dirichlet integral for a smooth function in a 2-dimensional domain transformed by area-preserving diffeomorphisms is equivalent to the problem of magnetic equilibrium of ideally conductive incompressible fluid in the same domain. In fact, the later problem is to solve the steady Euler equations, but it is quite difficult to find the solution directly, either by analytical methods or by numerical methods. However, the equivalence offers an efficient way to find the solutions numerically. We can minimize the Dirichlet integral numerically and the infimum is just the stream function to the velocity field of the steady Euler equations.

The minimization problem was solved by using 3 different numerical methods. The key point is to preserve areas. We use different penalty functions to guarantee this condition. The numerical results showss that the singularity formation was observed in all the cases. Every hyperbolic critical point of the original function gives rise to a singularity of the minimizer. We should note that the minimizing function is continuous, but its gradient is discontinuous along a segment of a curve. This phenomenon is called the $X - Y$ transition.

Although the work in my thesis is only a simplified model, it still implies the

existence of singularities. And the effect of the singularities is crucial in the plasma physics and astrophysics.

Appendix A

Adaptive Stepsize Method

The adaptive stepsize method is a very common technique to enhance the efficiency and accuracy of an algorithm in numerical analysis. Usually it is used for solving differential equations and computing integration. Let us consider an ordinary differential equation with initial value

$$y'(t) = f(t, y(t)), \quad y(t_0) = a \tag{A.1}$$

where $t \in [t_0, T]$. We want to approximate the value of $y(T)$. The simplest method to solve this problem is Euler's method. In this method, we use a set of points chosen on the interval $[t_0, T]$ and find the approximation value by iteration. Usually the stepsize h is fixed, say $h = (T - t_0)/N$ and then we define a recursive sequence as

$$y_{k+1} = y_k + hf(t_k, y_k) \tag{A.2}$$

where $t_k = t_0 + kh$, $0 \leq k \leq N$. By the Taylor series, we know

$$y(x + h) = y(x) + hf(x, y(x)) + f'(\theta, y(\theta))\frac{h^2}{2} \tag{A.3}$$

where $\theta \in [x, x+h]$. Since $f'(\theta, y(\theta))$ is a constant, then the stepsize h decides the accuracy of the approximation. In other words, as h decreases, the algorithm yields more precise results. If the error

$$\epsilon = |y(t_0 + kh) - y_k| \tag{A.4}$$

is bigger than the allowed error ϵ_t, we have to decrease h. If ϵ is much smaller than ϵ_t, we can raise h a little.

In our example (FEM), we can use the adaptive stepsize method during the process of minimization. Actually, the stepsize h decides how long the grid points move along the opposite direction of the gradients. We use the following rule to modify the stepsize,

if $|E_{k+1} - E_k| < 10^{-6}$, $h = h \times 1.01$

if $|E_{k+1} - E_k| > 10^{-6}$, $h = h \times 0.7$

where E_k and E_{k+1} denote the energies of two consequent steps. We should note that the second condition implies instability, so we should use the grid points of the last step, instead of the current step, after modifying of h.

Appendix B

Fast Fourier Transform

The Fast Fourier Transform (FFT) is a method to compute the Discrete Fourier Transform (DFT), which transforms a sequence of complex number into components of different frequencies, as well the inverse of DFT. DFT is an important technique in various digital signal processing applications, such as linear filtering, correlation analysis, and spectrum analysis. In our case, we use DFT to eliminate the oscillation during the minimization and make the grid points move more smoothly.

Let $\{x_i,\, 0 \leq i \leq N\}$ be a sequence of complex numbers. The DFT is defined by the formula

$$X_i = \sum_{j=0}^{N} x_i e^{-i2\pi k \frac{j}{N}} \quad 0 \leq i \leq N. \tag{B.1}$$

It takes $O(N^2)$ arithmetical operations to compute the DFT of N points. The FFT computes the same results more quickly. The FFT only needs $O(N \log N)$ arithmetical operations to compute the same problem. There are many distinct FFT algorithms and most of them depend on the factorization of N. Thus, N should not be a prim number.

In our example, we take FFT for each row of the matrices X and Y. We double the length of each row by reflection to guarantee N to be a composite of two numbers. For convenience, we use the built-in functions `fft` and `ifft` in Matlab. The functions

`Y = fft(x)` and `y = ifft(X)` implement the transform and inverse transform pair given for vectors of length N by

$$X(k) = \sum_{j=1}^{N} x(j)\omega_N^{(j-1)(k-1)} \tag{B.2}$$

$$x(j) = \frac{1}{N}\sum_{k=1}^{N} X(k)\omega_N^{-(j-1)(k-1)} \tag{B.3}$$

where ω_N is an N-th root of unity

$$\omega_N = e^{\frac{-2\pi}{N}i}. \tag{B.4}$$

We should note that the results of `fft` and `ifft` are both vectors of complex numbers and we only need the real part of the entries in the vectors.

Bibliography

[1] V. I. Arnold and B. Khesin, *Topological Methods in Hydrodynamics*, (Springer, 1998)

[2] C. Machioro and M. Pulvirenti, *Mathematical theory of incompressible nonviscous Fluids*, (Springer, 1994)

[3] A. Majda and A. Bertozzi, *Vorticity and Incompressible Flow*, (Cambridge University Press, 2002)

[4] R. Kulsrud, *Plasma Physics for Astrophysics*, (Princeton University Press, 2004)

[5] A. Long and D. N. Sedley, *Epicureanism: The principals of conservation, the Hellenistic Philosophers, Vol 1: Translations of the principal sources with philosophical commentary*, (Cambridge University Press, 1987)

[6] J.C. Heinrich and R.S. Marshall, *Viscous incompressible flow by a penalty function finite element method*, Computers and Fluids Vol 9, p. 73-83, March 1981

[7] J.N. Reddy, *An Introduction to Nonlinear Finite Element Analysis*, (Oxford University Press, 2004)

[8] T. Iwaniec and G. Martin, *Transformation groups in differential geometry*, (Springer, 2001)

[9] L.C. Evans, *Partial Differential Equations*, (American Mathematical Society, 1998)

[10] J. Freidberg, *Ideal Magnetohydrodynamics*, (Springer, 1987)

[11] P. Sturrock, *Plasma physics: an introduction to the theory of astrophysical, geophysical, and laboratory plasma*, (Cambridge University Press, 1994)

[12] Shih-I Pai, *Magnetogasdynamics and Plasma Dynamics*, (Cambridge University Press, 1962)

[13] R.D. Blandford and K. S. Thorne, *Lecture notes of the course, application of classical physics*, unpublished

[14] V. Arnold, *Mathematical Methods of Classical Mechanics (2nd ed.)*, (Springer, 1989)

[15] P. Lawrence and E. Stredulinsky, *Two dimensional Magnetohydrodynamic Equilibria with prescribed topology*, Communications on Pure and Applied Mathematics, Vol. 53, Issue 9, p.1177-1200, September 2000

[16] A. Iserles, *A First Course in the Numerical Analysis of Differential Equations* (Cambridge University Press, 1996)